https://doi.org/10.1093/plcell/koac270 THE PLANT CELL 2022: 34: 4816–4839

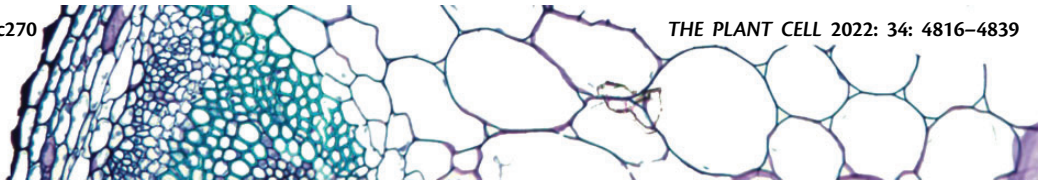

Research Article

Strigolactones act downstream of gibberellins to regulate fiber cell elongation and cell wall thickness in cotton (*Gossypium hirsutum*)

Zailong Tian ,[1] Yuzhou Zhang ,[2,3] Liping Zhu ,[1] Bin Jiang ,[1] Huiqin Wang ,[1] Ruxi Gao ,[2] Jiří Friml [3] and Guanghui Xiao [1,*]

1 College of Life Sciences, Shaanxi Normal University, Xi'an, China
2 College of Life Sciences, Northwest A&F University, Shaanxi, Yangling, China
3 Institute of Science and Technology Austria, 3400 Klosterneuburg, Austria

*Author for correspondence: guanghuix@snnu.edu.cn
These authors contributed equally (Y.Z. and Z.T.).
G.X. and Y.Z. designed the research; Z.T., L.Z., B.J., W.H., and G.R. performed the research and analyzed the data; Y.Z., G.X., and J.F. wrote and revised the manuscript.
The authors responsible for distribution of materials integral to the findings presented in this article in accordance with the policy described in the Instructions for Authors (https://academic.oup.com/plcell) are: Guanghui Xiao (guanghuix@snnu.edu.cn) and Yuzhou Zhang (yuzhou.zhang@ist.ac.at).

Abstract

Strigolactones (SLs) are a class of phytohormones that regulate plant shoot branching and adventitious root development. However, little is known regarding the role of SLs in controlling the behavior of the smallest unit of the organism, the single cell. Here, taking advantage of a classic single-cell model offered by the cotton (*Gossypium hirsutum*) fiber cell, we show that SLs, whose biosynthesis is fine-tuned by gibberellins (GAs), positively regulate cell elongation and cell wall thickness by promoting the biosynthesis of very long-chain fatty acids (VLCFAs) and cellulose, respectively. Furthermore, we identified two layers of transcription factors (TFs) involved in the hierarchical regulation of this GA–SL crosstalk. The top-layer TF GROWTH-REGULATING FACTOR 4 (GhGRF4) directly activates expression of the SL biosynthetic gene *DWARF27* (*D27*) to increase SL accumulation in fiber cells and GAs induce *GhGRF4* expression. SLs induce the expression of four second-layer TF genes (*GhNAC100-2*, *GhBLH51*, *GhGT2*, and *GhB9SHZ1*), which transmit SL signals downstream to two ketoacyl-CoA synthase genes (*KCS*) and three cellulose synthase (*CesA*) genes by directly activating their transcription. Finally, the KCS and CesA enzymes catalyze the biosynthesis of VLCFAs and cellulose, respectively, to regulate development of high-grade cotton fibers. In addition to providing a theoretical basis for cotton fiber improvement, our results shed light on SL signaling in plant development at the single-cell level.

Introduction

Cotton (*Gossypium hirsutum*) fibers are single-celled trichomes derived from ovule epidermis cells, and are a classic model for studying cell elongation and cell wall biosynthesis (Kim and Triplett, 2001; Huang et al., 2021). Cotton fiber cell development can be divided into five overlapping stages: cell initiation, elongation, transitional wall thickening, cell wall thickening, and maturation (Haigler et al., 2012). Cell elongation and secondary cell wall biosynthesis determine cell length and strength, which largely contribute to the economic value of the cotton fiber (Tausif et al., 2018). Upland cotton (*G. hirsutum*) produces high-grade cotton fibers that

Received January 20, 2022. Accepted August 25, 2022. Advance access publication August 30, 2022

Open Access

IN A NUTSHELL

Background: The strigolactone (SL) plant hormones regulate plant architecture, including shoot branches and adventurous roots. However, the role of SLs in shaping plant cell morphology is still undetermined. Cotton (*Gossypium hirsutum*) fibers are single-celled trichomes derived from ovule epidermal cells and are excellent models to study plant cell development. Therefore, we used cotton fibers to explore the role of SLs in plant cell development and the mechanistic framework involved in this biological process.

Question: How do SLs regulate cotton fiber cell growth? What are the regulatory mechanism underlying the SL-mediated fiber cell development?

Findings: SLs enhance cotton fiber cell elongation and cell wall thickness to simultaneously promote length and strength of fiber cells. Furthermore, we identified a cluster of transcription factors that transmit SL signals downstream to the genes related to the biosynthesis of very-long-chain fatty acid and cellulose, the two components essential for the fiber cell elongation and cell wall thickening. Moreover, the accumulation of SLs in fiber cells relies on the gibberellin-promoted expression of the SL biosynthesis gene *DWARF27*, suggesting that the phytohormone GA acts upstream of SLs in cotton fiber cell development.

Next steps: For fiber cell development, cell elongation and secondary cell wall thickening generally act antagonistically. Therefore, identifying mechanisms by which the SLs promote fiber cell elongation without the penalty of decreasing the secondary cell wall thickness remains an open question for future research.

are long and robust, making it one of the most important economic crops worldwide, as it provides the world's largest source of natural fiber for the global textile industry.

Cell walls are composed of primary and secondary layers. The biosynthesis of primary cell walls is associated with cell elongation, while the biosynthesis of secondary cell walls closely correlates with cell wall thickness (Cosgrove and Jarvis, 2012; Houston et al., 2016). The primary cell wall, a relatively thin, pliant, and highly hydrated structure, is extensible to allow wall stress relaxation, promoting cell water uptake and physical enlargement and elongation of cells. These features allow the incorporation of newly deposited wall polymers into the load-bearing structures of the primary cell wall for cell elongation (Hamant and Traas, 2010). The secondary cell wall, however, needs to exhibit compressive as well as tensile strength, but not extensibility, to provide strength and rigidity to plant tissues that have usually ceased growing. Plant hormones (auxin, brassinosteroids, gibberellins (GAs), and ethylene) present in relatively low concentrations have essential roles in the development of plant cells, including cotton fiber cells (Sun et al., 2005; Yang et al., 2014; Li et al., 2015;Zeng et al., 2019; Xiao et al., 2019). Among these phytohormones, GAs are one of the most studied in cotton fiber development, because they regulate the initiation, elongation, and secondary cell wall thickness of fiber cells. Enhancing GA accumulation in cotton fibers by exogenous application of GA or endogenous overexpression of the GA biosynthetic gene *Gibberellin 20-oxidase1* (*GhGA20ox1*) promotes fiber cell initiation and elongation, leading to bushy and longer fibers around the ovule surface. Conversely, treatment with the GA biosynthesis inhibitor paclobutrazol (PAC) results in sparse and short fibers (Xiao et al., 2010). DELLA proteins are negative regulators in the GA signaling pathway. Mechanistically, the cotton DELLA protein Slender rice 1 (GhSLR1) specifically interacts with the transcription factor (TF) GhHOX3 (Homeodomain protein 3) to inhibit the expression of downstream genes related to fiber elongation (Shan et al., 2014). With high GA levels, GhSLR1 is degraded to release GhHOX3 and activate the expression of target genes to promote fiber elongation. In addition to regulating cotton fiber initiation and elongation, GA also promotes secondary cell wall development in cotton fibers, which is achieved by upregulating the expression of sucrose synthase genes (Bai et al., 2014; Xiao et al., 2016). Despite some advances in clarifying the function of GA in cotton fiber cell elongation and secondary cell wall biosynthesis, the GA regulatory network underlying these cellular biological processes is still unknown.

Strigolactones (SLs), first isolated from cotton root exudates in 1966 (Cook et al., 1966), were later recognized as a new class of plant hormones (Gomez-Roldan et al., 2008; Umehara et al., 2008; Khosla and Nelson, 2016). SLs are synthesized from the key precursor carlactone , which is derived from all-trans β-carotene via the action of an isomerase DWARF 27 (D27) and two carotenoid cleavage dioxygenases (CCD7 and CCD8) (Mashiguchi et al., 2021). SLs have diverse functions across plants, especially in the regulation of important agronomical traits such as shoot branching, adventitious rooting, and parasitic weed infections (Gomez-Roldan et al., 2008; Rasmussen et al., 2012; Brewer et al., 2013). Moreover, SLs regulate the elongation of root hairs in Arabidopsis (*Arabidopsis thaliana*) (Koltai et al., 2010; Kapulnik et al., 2011), which is also a single-cell model similar to cotton fiber cell. However, whether SLs are also involved in cotton fiber elongation to generally regulate plant cell elongation is still unknown, and the regulatory mechanism of SLs in plant cell elongation remains elusive.

Phytohormone synergy and signaling interdependency, namely phytohormone crosstalk, is ubiquitous in the regulation of plant development at the single-cell level (Vanstraelen and Benková, 2012). In cotton, cytokinin disrupts auxin accumulation mediated by the auxin efflux carrier PIN-FORMED 3a in the ovule epidermis to inhibit fiber initiation, suggesting that cytokinin–auxin crosstalk is involved in regulating fiber cell initiation (Zeng et al., 2019). Nevertheless, knowledge regarding the involvement of phytohormone crosstalk in fiber cell elongation and secondary cell wall thickening is still scarce.

In this study, we describe the positive effect of SLs on regulating fiber cell elongation and secondary cell wall thickness, and identify a series of key TFs that transmit the SL signal to the downstream genes related to cell elongation and secondary cell wall thickness. Additionally, we show that SL biosynthesis in fiber cells is positively regulated by GA signaling, and identify the key TF GROWTH-REGULATING FACTOR 4 (GhGRF4), which mediates GA-induced SL biosynthesis, suggesting that SL acts downstream of GA signal in fiber cell elongation and secondary cell wall thickness. Together, we not only uncovered the mechanistic framework for the individual phytohormone SLs and GA in shaping fiber cell length and secondary cell wall thickness, but also revealed the participation of GA–SL crosstalk in the development of this single-cell model, enabling us to comprehensively understand the regulatory network of phytohormones in plant development at the single-cell level.

Results

SLs positively regulate cotton fiber cell elongation

To understand the role of SLs in cotton fiber cell development, we analyzed SL contents along the developmental trajectory of the cotton fiber. We showed that 2′-*epi*-5-deoxystrigol (*epi*-5DS), a canonical endogenous SL (Seto et al., 2014), is essentially undetectable in fibers at the initiation stage, approximately 0- to 5-day postanthesis (DPA) (Figure 1A). However, the content of *epi*-5DS increased gradually during the fiber elongation stage (around 5–20 DPA) (Figure 1A). Consistently, reverse transcription–quantitative PCR (RT–qPCR) analysis of SL biosynthesis genes demonstrated that *D27* relative expression levels are significantly higher in fibers during the elongation stages (around 5–20 DPA) compared to fibers at the initiation stages (0–5 DPA). Additionally, the relative expression levels of *MORE AXILLARY GROWTH 1* (*MAX1*), *MAX3*, and *MAX4* increase significantly during the fiber elongation stages (10 and 20 DPA) (Supplemental Figure S1, A and B). These results indicated that increased SL biosynthesis may be involved in cotton fiber elongation.

To confirm the function of SLs in cotton fiber development, we used an in vitro ovule culture system to investigate the growth of cotton fibers in response to GR24 (a synthetic analog of SL, rac-GR24) and Tis108 (an established SL biosynthesis inhibitor) (Besserer et al., 2008; Ito et al., 2013). Compared to the untreated control, 15-μM GR24 treatment significantly promoted cotton fiber elongation, while 10-μM Tis108 strongly inhibited elongation (Figure 1, B and C). We established that *G. hirsutum* has six *GhD27* genes, and the member (Gh_D11G1134) used in this study was highly expressed in multiple tissues, including fiber cells (Supplemental Figure S2). In addition, we developed two transgenic cotton lines in which the key SL biosynthesis gene *GhD27* (Gh_D11G1134), encoding a β-carotene isomerase, was either overexpressed or knocked out via genome editing (Figure 1D; Supplemental Figures S3 and S4). Overexpression of *GhD27* (*GhD27*-OE) under the control of the cauliflower mosaic virus 35S promoter resulted in increased *epi*-5DS contents in fibers (Figure 1E; Supplemental Figure S5), leading to larger cotton bolls and much longer cotton fibers when compared to the WT (Figure 1,G–I). In contrast, the *GhD27*-knockout line (*Ghd27-ko*), generated by clustered regularly interspaced short palindromic repeats (CRISPR)-associated nuclease 9 (Cas9)-mediated genome editing, showed more branches, reduced plant height, smaller cotton bolls, and shorter fibers along with a significant decrease in the level of *epi*-5DS compared to WT (Figure 1, E–I; Supplemental Figures S5 and S6). Additionally, exogenous application of GR24 rescued the shortened fibers of *Ghd27-ko* transgenic cotton, suggesting that its short fiber phenotype results from its decreased level of SLs (Supplemental Figure S7). These in vitro and *in planta* experimental results show that the plant hormone SL promotes cotton fiber development.

SLs activate KCS-mediated very long-chain fatty acid biosynthesis to promote fiber cell elongation

To uncover the components or signaling pathways involved in SL-mediated cotton fiber elongation, we performed a transcriptome deep sequencing (RNA-seq) analysis of cotton fibers subjected to either 15-μM GR24 or 10-μM Tis108 treatment at 10 DPA. Hierarchical clustering showed that the differential expression of 9,052 genes between GR24 and Tis108 treatments was closely associated with the SL signaling cascade (Figure 2A; Supplemental Figure S8A and Supplemental Data Set 1). Kyoto Encyclopedia of Genes and Genomes (KEGG) pathway enrichment analysis revealed that these differentially expressed genes (DEGs) are enriched for functions related to fatty acid-related pathways, with a pronounced enrichment for genes involved in fatty acid elongation (Figure 2B; Supplemental Data Set 2).

Among fatty acids, very-long-chain fatty acids (VLCFAs), whose biosynthesis is catalyzed by ketoacyl-CoA synthase (KCS), promote cotton fiber elongation (Qin et al., 2007; Wang et al., 2017). In line with the transcriptome results (Supplemental Figure S8B), RT–qPCR analysis confirmed that the expression levels of four *KCS* genes (*KCS5*, *KCS13*, *KCS23*, and *KCS57*) are upregulated by GR24 treatment but downregulated after Tis108 treatment (Figure 2C). Correspondingly, the levels of two VLCFAs, C22:0 and C26:0, were significantly increased in cotton fibers treated with GR24 but decreased after Tis108 treatment (Figure 2D). Consistently, compared

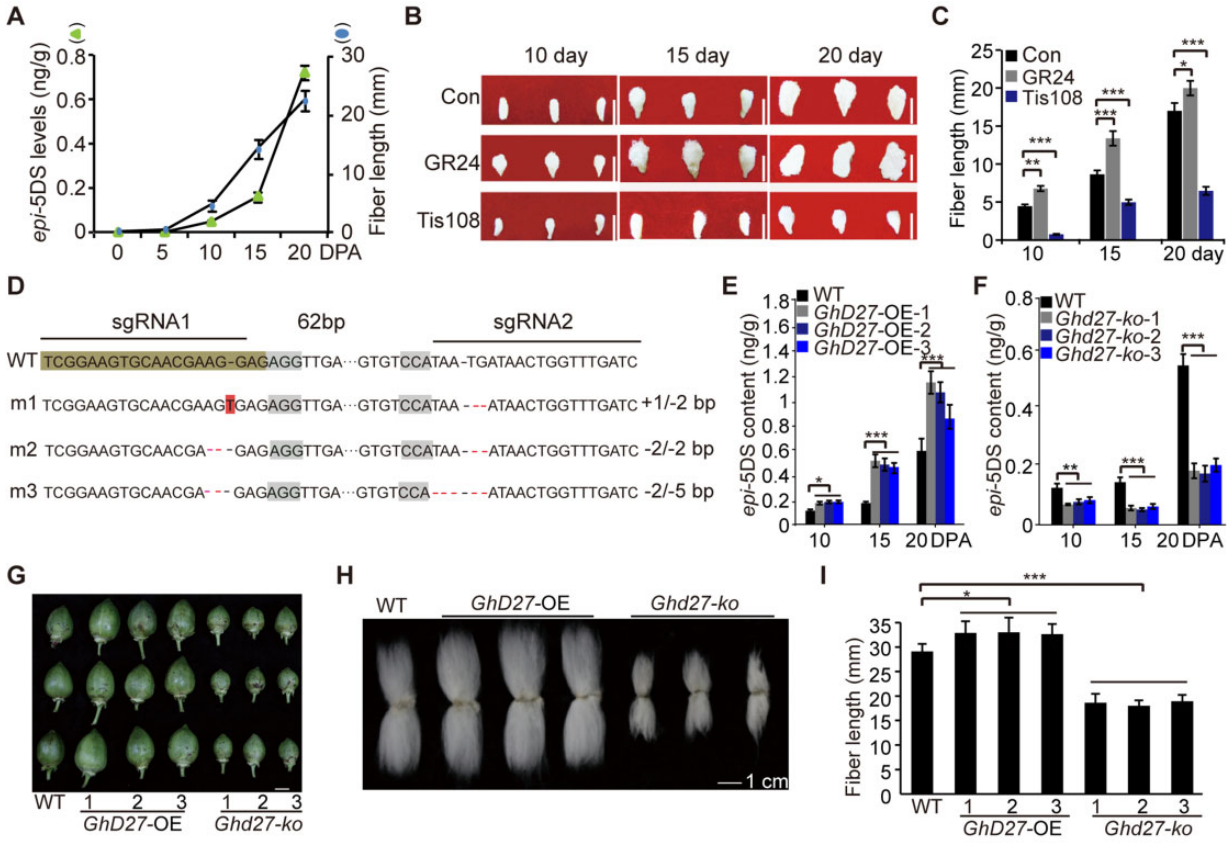

Figure 1 SLs promote cotton fiber cell elongation. A, Contents of the canonical SL *epi*-5DS in cotton fibers at different growth stages. B, Phenotypes of cotton fibers (collected at 1 DPA) cultured in vitro on medium containing 15 μM of the synthetic SL analog GR24 or 10 μM of the SL biosynthesis inhibitor Tis108 for 10, 15, or 20 days. Con, untreated control. Scale bars, 5 mm. C, Mean fiber length in (B). D, Sanger sequencing-based genotyping of *GhD27* knockout lines obtained by CRISPR/Cas9-mediated gene editing. The edited gene, *GhD27* (Gh_D11G1134), is from D-subgenome of Upland cotton. Nucleotide deletions are indicated by the red dashes, and the insertion in line m1 is indicated by a "T" highlighted in red. The sgRNA-matching sites are located at the first exon of *GhD27*. E, *epi*-5DS contents of 10-, 15-, and 20-DPA cotton fibers collected from the WT and *GhD27*-OE transgenic lines. F, *epi*-5DS contents of 10-, 15-, and 20-DPA cotton fibers collected from the WT and the *GhD27* knockout line (*Ghd27-ko*). G, Images of 25-DPA cotton bolls from WT, *GhD27*-OE, and *Ghd27-ko* transgenic plants. Scale bar, 1 cm. H, Representative images of mature fibers from WT, *GhD27*-OE, and *Ghd27-ko* transgenic plants. Scale bar, 1 cm. I, Mean length of mature fibers in (H). A total of 25 naturally open bolls were harvested from each line. Fiber of 10–15 g from each sample was measured by the HVI1000 automatic fiber testing system. Data are means ± SD from three independent experiments. Statistical significance was determined using one-way analyses of variance (ANOVA) combined with Tukey's test. $^*P < 0.05$; $^{**}P < 0.01$; $^{***}P < 0.001$. Con, untreated fibers. WT (jin668).

to the WT, the RNA-seq and RT–qPCR analysis showed significantly higher expression levels for the four *KCS* genes in transgenic cotton line *GhD27*-OE (Figure 2E; Supplemental Figure S8C), with a corresponding significant increase in C22:0 and C26:0 levels in fibers from *GhD27*-OE plants (Figure 2F). Furthermore, the relative expression levels of these four *KCS* genes in the knockout line *GdD27-ko* were significantly downregulated, resulting in lower levels of C22:0 and C26:0 in fiber cells (Figure 2, E and F). These results indicate that SLs promote cotton fiber elongation by promoting KCS-mediated VLCFA biosynthesis.

SLs promote CesA-dependent cellulose biosynthesis to enhance fiber cell wall thickness

Cellulose, the world's most abundant biopolymer and a key structural component of the plant cell wall, is synthesized at the plasma membrane by cellulose synthase (CesA) to control secondary cell wall thickness (Polko and Kieber, 2019; Purushotham et al., 2020). Pontamine fast scarlet 4B (S4B) dye and calcofluor white are widely used to stain cellulose and indicate the cell wall thickness (Huang et al., 2016). Electron microscopy examinations of semi-thin sections prepared from fiber cells closest to the ovule epidermal layer verified that fiber cell is significantly thicker following GR24 treatment, and significantly thinner after Tis108 application compared to untreated controls (Figure 3, A–E; Supplemental Figure S9). Gene Ontology (GO) enrichment analysis of DEGs from the three sets of transcriptomes (control, GR24-treated, and Tis108-treated) revealed that cell wall-associated genes are enriched after GR24 treatment (Figure 3F; Supplemental Table S1). These results indicated dual functions for SL in fiber development: besides promoting fiber cell elongation, SLs also enhance secondary cell wall thickness.

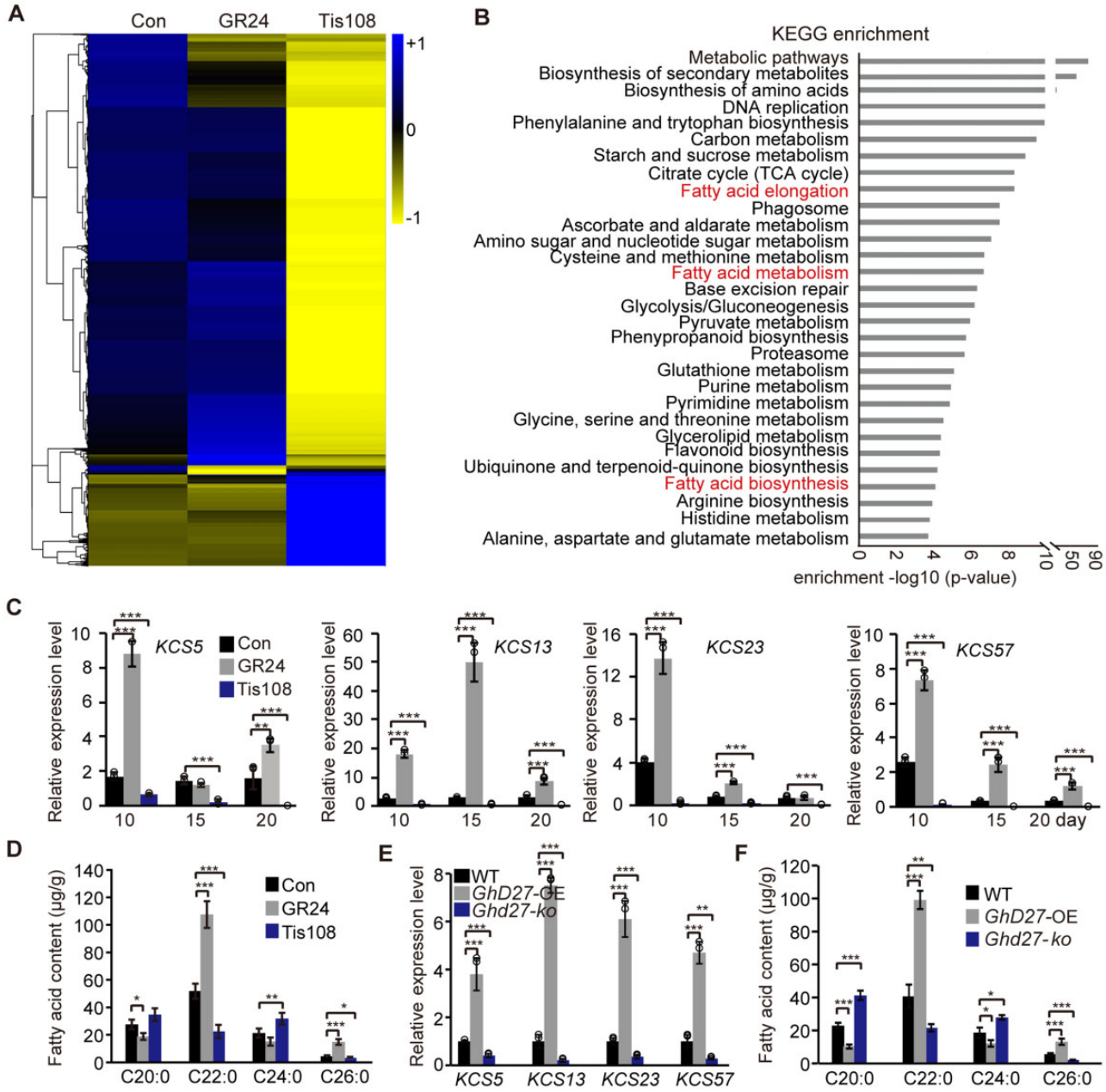

Figure 2 SL positively regulates KCS-mediated VLCFA biosynthesis. A, Heatmap representation of the expression from DEGs in untreated cotton fibers (Con) and in fibers treated with 15-μM GR24 or 10-μM Tis108 for 10 days. The scale bar indicates the *Z*-score normalized fragment per kilobase of transcript per million mapped reads value. The heatmap was constructed using R4.0.5. B, Enrichment of KEGG pathway terms for genes upregulated by GR24 treatment and downregulated by Tis108 treatment. Analysis was conducted using the KOBAS version 3.0 web server. C, Relative expression levels of *GhKCS5*, *GhKCS13*, *GhKCS23*, and *GhKCS57* in untreated cotton fibers (Con) and fibers treated with 15-μM GR24 or 10-μM Tis108 for 10, 15, or 20 days. D, Contents for VLCFA (including C20:0, C22:0, C24:0, and C26:0) in untreated cotton fibers and those treated with 15-μM GR24 or 10-μM Tis108 for 10 days, as determined by liquid chromatography–mass spectrometry (LC–MS). E, Relative expression levels of *GhKCS5*, *GhKCS13*, *GhKCS23*, and *GhKCS57* in 10-DPA fibers from WT, *GhD27*-OE, and *Ghd27-ko* transgenic cotton plants. F, VLCFA contents in 10-DPA fibers from WT, *GhD27*-OE, and *Ghd27-ko* transgenic plants. Data are means ± SD from three independent experiments. Statistical significance was determined using one-way ANOVA combined with Tukey's test. $^{*}P < 0.05$; $^{**}P < 0.01$; $^{***}P < 0.001$. Con, untreated fibers. WT (jin668).

Consistent with the transcriptome results, RT–qPCR analysis confirmed that the four *CesA* genes (*CesA8*, *CesA4*, *CesA7-1*, and *CesA7-2*), responsible for the secondary cell wall cellulose biosynthesis (Huang et al., 2021), are strongly and significantly upregulated following GR24 treatment (Figure 3G), leading to increased accumulation of cellulose in fiber cell walls (Figure 3H). In contrast, application of Tis108 resulted in downregulated expression of these four *CesA* genes and decreased cellulose accumulation in fibers (Figure 3, G and H).

Moreover, we investigated the fiber cell wall thickness in three independent lines each for *GhD27*-OE transgenic

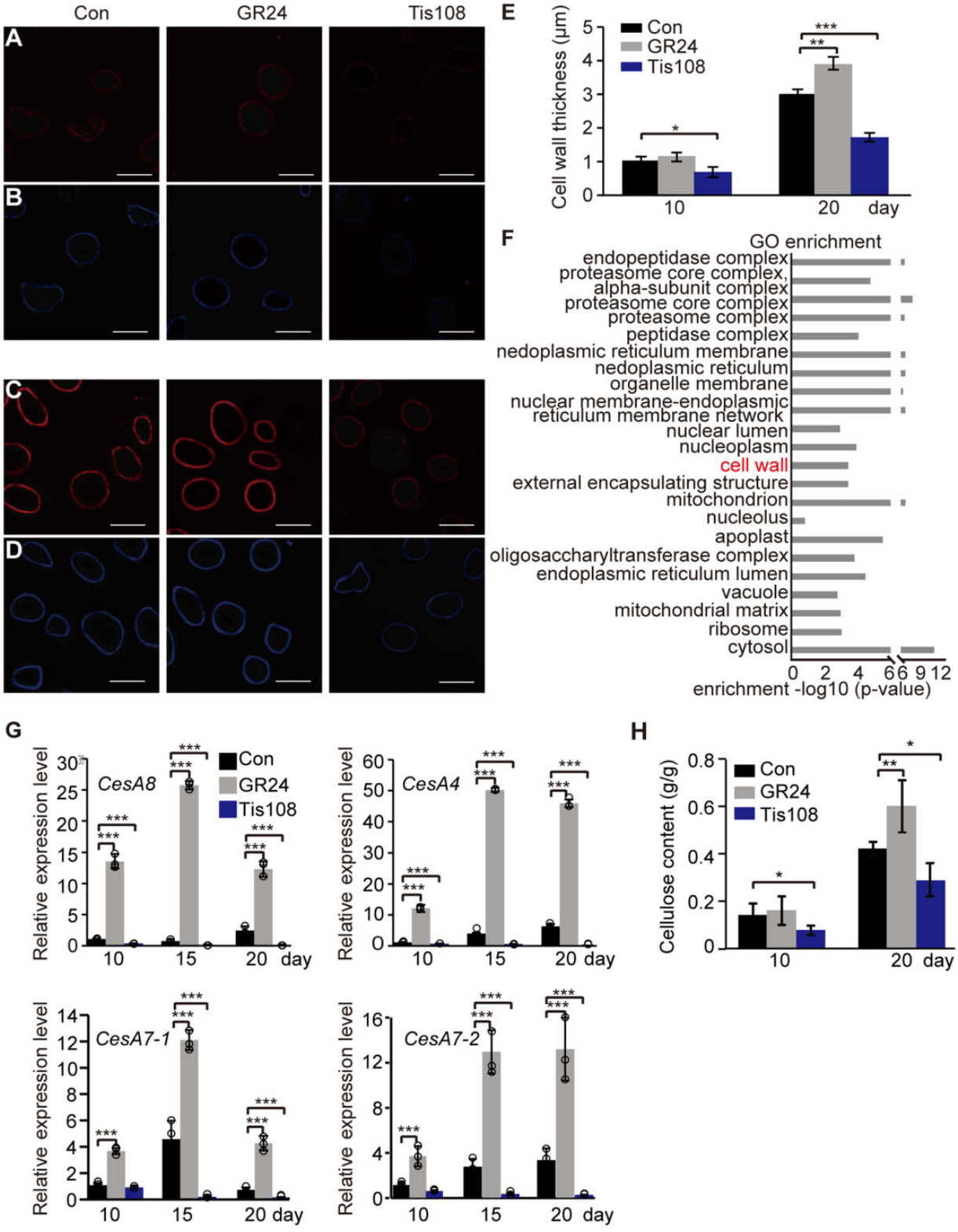

Figure 3 SL treatment promotes fiber cell wall thickness by positively regulating *CesA*-mediated cellulose biosynthesis. A–D, Cross-sections of paraffin-embedded fiber cells grown in vitro for 10 or 20 days from untreated (Con) and treated fibers with either GR24 or Tis108 following staining with Pontamine Fast S4B (A and C) or calcofluor white (B and D). (A and B Fiber cells cultured in vitro for 10 days. C and D Fiber cells cultured in vitro for 20 days. Scale bars, 20 μm. E, Mean cell wall thickness in untreated fibers and those treated with either GR24 or Tis108 in (B) and (D). The sections were photographed under a confocal laser scanning microscope TCS SP5 (Leica, Wetzlar, Germany) and then the cell wall thickness was measured with the Motic Images Plus version 3.0 software. Thirty fibers from three ovules were used for each sample, and each fiber was measured 3 times. F, GO enrichment analysis of genes upregulated in response to GR24 treatment but downregulated by Tis108 treatment in cotton

(continued)

cotton and *Ghd27-ko* by semi-thin section analysis at three representative developmental stages, namely fiber cell elongation (10 DPA), fiber cell wall thickening (20 DPA and 30 DPA), and fiber cell maturation (>45 DPA). We established that overexpression of *GhD27* increases, while knocking out *GhD27* reduces, cell wall thickness of fibers at all three developmental stages (Figure 4A; Supplemental Figures S10 and 11). Similarly, RNA-seq and RT–qPCR analysis showed higher expression levels for the four *CesA* genes and much higher accumulation of cellulose in the *GhD27*-OE overexpressing line (Figure 4, B and C; Supplemental Figure S12). Conversely, the expression of *CesA* genes in the *Ghd27-ko* line was significantly downregulated (Figure 4C), resulting in the lower cellulose content of fiber cells (Figure 4B). These results demonstrate that in addition to KCS-mediated VLCFA biosynthesis for fiber elongation, SLs also regulate CesA-dependent cellulose biosynthesis to modulate fiber cell wall thickness.

Moreover, we treated cotton fibers with 2, 6-dichlorobenzonitrile (DCB) and coumarin, which were reported to be the most effective and specific inhibitors for cellulose biosynthesis (Martínez-Rubio et al., 2018). Either DCB or coumarin treatment significantly reduced the content of cellulose in fibers (Supplemental Figure S13A). However, the *epi*-5DS content and the expression of genes related to SL biosynthesis in DCB- or coumarin-treated fibers were comparable to those in fibers without any treatment (Supplemental Figure S13, B and C).

Identification of SL-inducible TF genes transmitting SL signals downstream to *KCS* and *CesA* genes

Our next objective was to identify potential components involved in the regulation of SL-mediated *CesA*/*KCS* gene expression. From a comparison between the transcriptome of untreated fibers and that of fibers treated with either 15-μM GR24 or 10-μM Tis108, we identified 19 TF genes showing strongly upregulated expression levels following GR24 treatment and downregulated after Tis108 treatment (Supplemental Table S2). Systematic yeast one-hybrid (Y1H) assays revealed that among these 19 TFs, 2 (GhB9SHZ1,

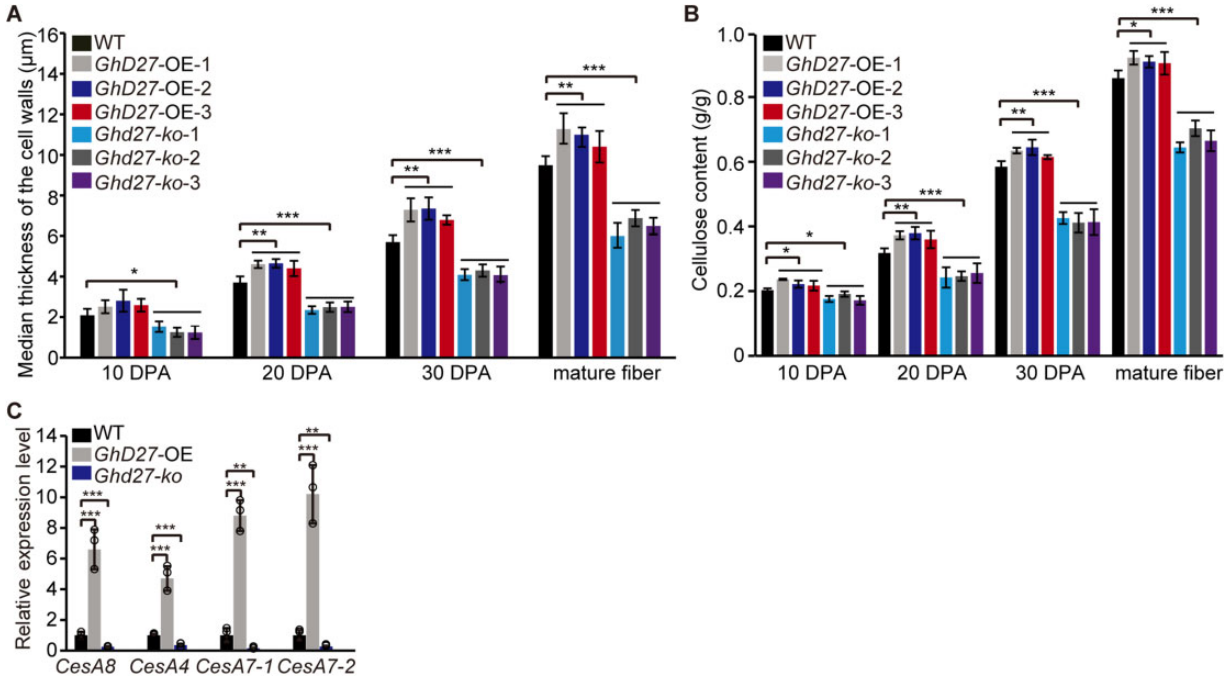

Figure 4 Analysis of fiber cell wall thickness, cellulose accumulation and relative expression levels of *GhCesA8*, *GhCesA4*, *GhCesA7-1*, and *GhCesA7-2* genes in WT, *GhD27*-OE, and *Ghd27-ko* transgenic plants. A, Mean cell wall thickness of fibers from WT, *GhD27*-OE, and *Ghd27-ko* transgenic plants as shown in Supplemental Figure S3. Thirty fibers from three ovules were used for each sample, and each fiber was measured 3 times. B, Cellulose content of fibers from WT, *GhD27*-OE, and *Ghd27-ko* transgenic plants. C, Relative expression levels of *GhCesA8*, *GhCesA4*, *GhCesA7-1*, and *GhCesA7-2* genes in fiber cells from WT, *GhD27*-OE and *Ghd27-ko* transgenic plants. Data are means ± SD from three independent experiments. Statistical significance was determined using one-way ANOVA combined with Tukey's test. *$P < 0.05$; **$P < 0.01$; ***$P < 0.001$.

Figure 3 (Continued)
fibers. GO functional enrichment analysis was performed using the ClueGO plugin version 2.5.6 in Cytoscape 3.6.1. G, Relative expression levels of *GhCesA8*, *GhCesA4*, *GhCesA7-1*, and *GhCesA7-2* in fibers treated with 15-μM GR24 or 10-μM Tis108 for 10, 15, or 20 days compared to untreated fibers. H, Cellulose contents between untreated fibers and those treated with 15-μM GR24 or 10-μM Tis108 for 10, 15, or 20 days. Data are means ± SD from three independent experiments. Statistical significance was determined using one-way ANOVA combined with Tukey's test. *$P < 0.05$; **$P < 0.01$; ***$P < 0.001$. Con, untreated fibers.

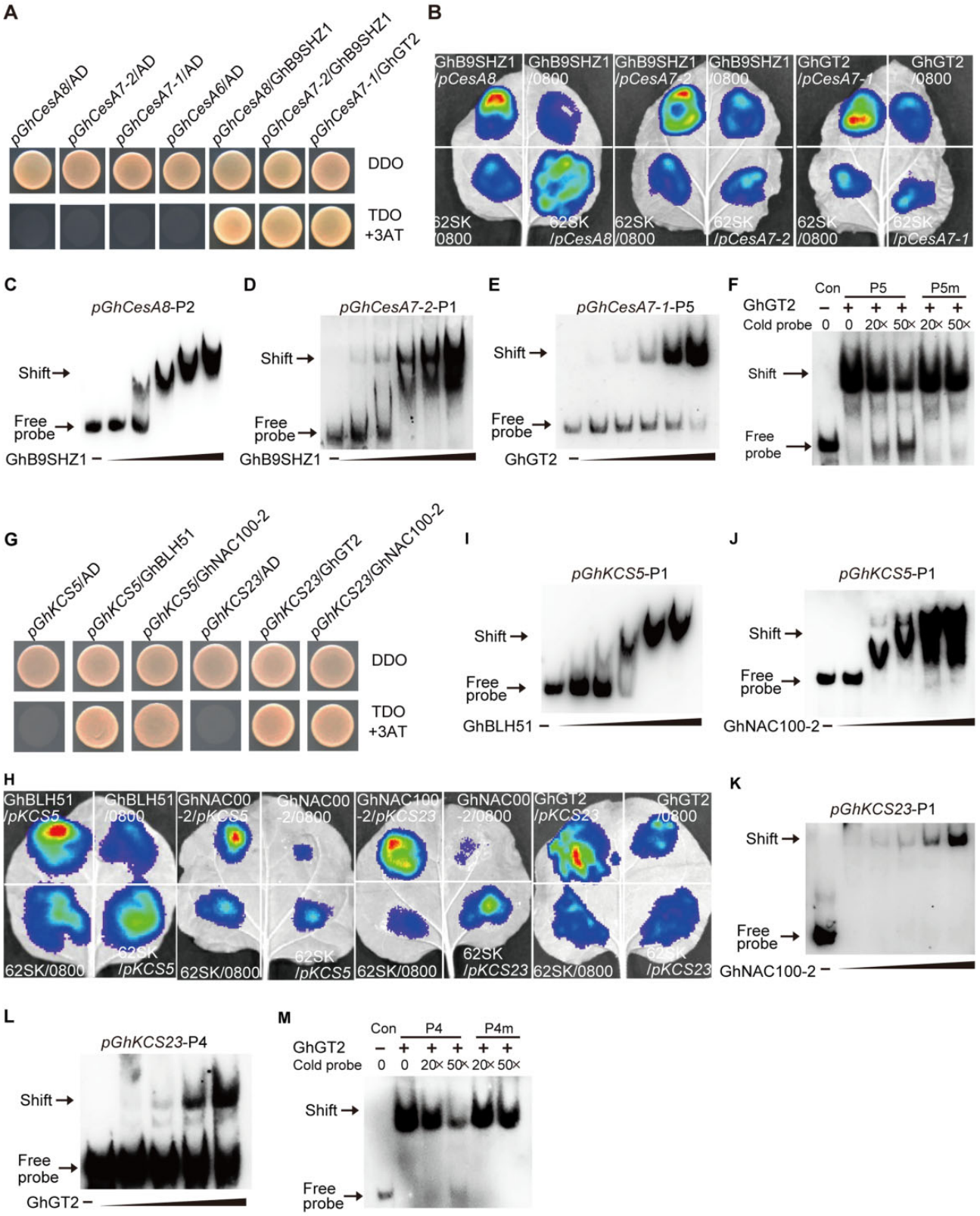

Figure 5 Identification of SL-inducible TF genes whose encoded proteins that directly activate the expression of *GhCesA* and *GhKCS* genes. A, Systematic Y1H assays showing the binding of the TFs GhB9SHZ1 to the *GhCesA8* and*GhCesA7-2* promoters, and of GhGT2 to the *GhCesA7-1* promoter. B, Transient infiltration assays in *N. benthamiana* leaves showing the transcriptional activation of the *LUC* reporter gene (under the control of the *GhCesA* promoter) by the corresponding SL-inducible TF genes as shown in (A). C–E, EMSA showing that GhB9SHZ1 directly binds to the P2 fragment of the *GhCesA8* promoter and the P1 fragment of the *GhCesA7-2* promoter, while GhGT2 directly binds to the P5 fragment of *GhCesA7-1* promoter. F, The biotin-labeled P5 fragment from the *GhCesA7-1* promoter was incubated with recombinant GhGT2 to compete with

(continued)

a C_2H_2 zinc finger TF and GhGT2, a plant trihelix DNA-binding protein) were capable of binding to the promoters of the three SL-inducible *CesA* genes (Figure 5A; Supplemental Figure S14). RT–qPCR analysis confirmed that the expression of *GhB9SHZ1* and *GhGT2* is strongly induced by GR24 but significantly decreased after Tis108 treatment (Supplemental Figure S15). More specifically, we observed that GhB9SHZ1 binds to the promoters of *CesA8* and *CesA7-2*, while GhGT2 bound to the *CesA7-1* promoter.

To experimentally confirm the DNA-binding activity and transcriptional regulation of GhB9SHZ1 toward *CesA8*/*CesA7-2* and of GhGT2 toward *CesA7-1*, we performed transient in vivo expression assays. Briefly, Agrobacterium (*Agrobacterium tumefaciens*) cultures harboring constructs expressing the gene encoding each TF driven by the 35S promoter, and the firefly luciferase (*LUC*) reporter gene driven by the *CesA8*/*CesA7-2*/*CesA7-1* promoters, were co-infiltrated into *Nicotiana benthamiana* leaves. In contrast to the empty vector control, co-expression of *GhB9SHZ1* or *GhGT2* with each *LUC* reporter construct enhanced the *LUC* reporter gene activity (Figure 5B; Supplemental Figure S16). We also investigated the binding region of the three *CesA* promoters targeted by GhB9SHZ1 or GhGT2 through both Y1H assays and electrophoretic mobility shift assays (EMSAs). The Y1H assay showed that GhB9SHZ1 can bind to the P2 fragment of the *CesA8* promoter and to the P1 fragment of the *CesA7-2* promoter (Supplemental Figure S17). The P5 fragment of the *CesA7-1* promoter was bound by GhGT2; importantly, this fragment contained a predicted GhGT2-binding site (Supplemental Figure S18). Furthermore, EMSA confirmed that recombinant GhB9SHZ1 has binding affinity for the P2 fragment of the *CesA8* promoter and the P1 fragment of the *CesA7-2* promoter (Figure 5, C and D), as did recombinant GhGT2 toward the P5 fragment of the *CesA7-1* promoter (Figure 5E). This binding affinity decreased gradually by adding increasing amounts of unlabeled intact probes but was not affected by adding increasing amounts of unlabeled mutated probes (Figure 5F).

We also identified three SL-inducible TFs, GhBLH51, GhNAC100-2, and GhGT2, that interact with *KCS* promoters (Figure 5G; Supplemental Figure S19). RT–qPCR analysis confirmed that these three TF genes are strongly induced by GR24 treatment but significantly downregulated after Tis108 treatment (Supplemental Figures S15 and S20). Specifically, we observed that GhBLH51 (a member of the BEL family of homeodomain proteins) and GhNAC100-2 (a member of the NAC TF family) bind to the *KCS5* promoter, while GhGT2 and GhNAC100-2 bind to the *KCS23* promoter. In contrast to the empty vector control, transient *in vivo* expression assays demonstrated that co-expression of *GhBLH51*, *GhNAC100-2*, or *GhGT2* with their appropriate *LUC* reporter constructs (based on Y1H assays) raises LUC activity (Figure 5H; Supplemental Figure S21). Furthermore, Y1H assays with truncated *KCS5* or *KCS23* promoters demonstrated that the binding region for GhBLH51 is in the P1 fragment of the *KCS5* promoter, while the binding site for GhNAC100-2 is in the P1 fragment of the *KCS5* and *KCS23* promoters (Supplemental Figures S22 and S23). The binding site for GhGT2 protein was located in the P4 fragment of the *KCS23* promoter, which contained a predicted GhGT2-binding site (Supplemental Figure S23). EMSA further confirmed that GhBLH51 has binding affinity for the P1 fragment of the *KCS5* promoter and that the GhNAC100-2 protein shows binding affinity for the P1 fragment of the *KCS5*/*KCS23* promoters (Figure 5, I–K). GhGT2 protein had binding affinity for the P4 fragment of the *KCS23* promoter (Figure 5L). This affinity decreased upon the addition of increasing amounts of unlabeled intact probes, but was not affected by adding increasing amounts of unlabeled mutated probes (Figure 5M).

To verify that the expression of the four identified TF genes capable of binding to the promoters of *CesA* and *KCS* was induced by SLs, we analyzed their expression levels in the transgenic cotton lines *GhD27*-OE and *Ghd27-ko*. Compared to the wild-type (WT), *GhB9SHZ1*, *GhBLH51*, *GhNAC100-2*, and *GhGT2* showed much higher expression levels in *GhD27*-OE, and much lower expression in *Ghd27-ko* (Supplemental Figure S24), suggesting that they are SL-inducible TF genes.

In summary, we identified four SL-inducible TF genes whose encoded proteins can bind to the promoters of the *CesA* and *KCS* genes to activate their expression, which in turn regulates the biosynthesis of cellulose and VLCFAs to modulate cotton fiber strength and length, respectively.

Silencing SL-inducible TF genes inhibits fiber cell elongation and cell wall thickness

To explore the role of the identified SL-inducible TFs in fiber development, we used virus-induced gene silencing (VIGS) experiments to knock down their transcript levels and analyzed the resulting phenotypes. To this end, we inserted specific fragments of around 500 bp representing the conserved

Figure 5 (Continued)
different concentrations of the cold probes (without biotin-label) of intact or mutated GT2 binding site. G, Y1H assays showing the binding of GhNAC100-2 to the *GhKCS5* and *GhKCS23* promoters, of GhBLH51 to the *GhKCS5* promoter, and of GhGT2 to the *GhKCS23* promoter. H, Transient infiltration assays in *N. benthamiana* leaves showing the transcriptional activation of the *LUC* reporter gene (under the control of the *GhKCS* promoters) by the corresponding SL-inducible TF genes shown in (G). I, EMSA showing that GhBLH51 directly binds to the P1 fragment of the *GhKCS5* promoter. J and K, EMSA showing that GhNAC100-2 directly binds to the P1 fragment of the *GhKCS5* and *GhKCS23* promoters. L, EMSA showing that GhGT2 directly binds to the P4 fragment of the *GhKCS23* promoter. M, The biotin-labeled P4 fragment from *GhKCS23* promoter was incubated with recombinant GhGT2 to compete with different concentrations of the cold probes (without biotin-label) of intact or mutated GT2 binding site (P4m).

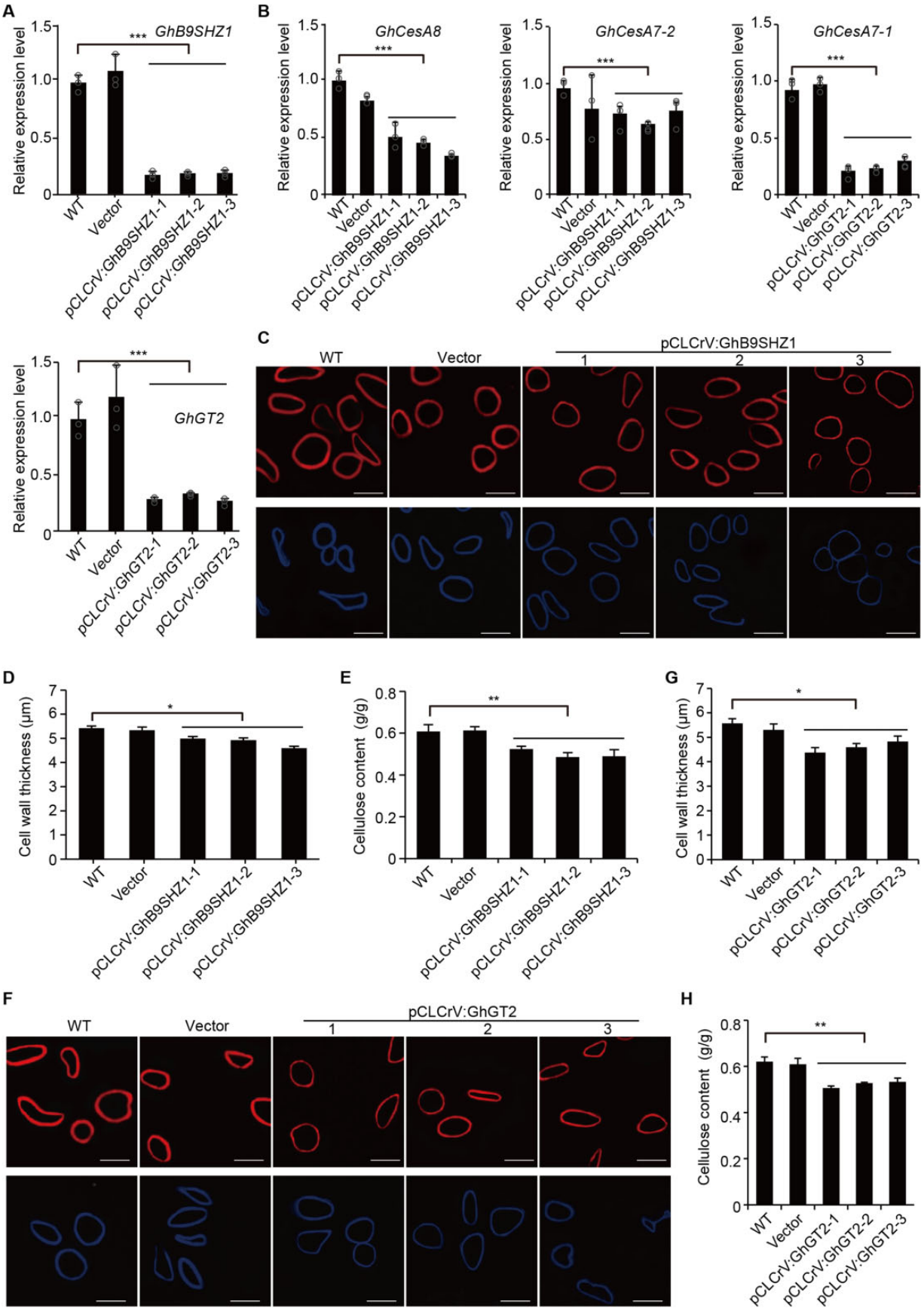

Figure 6 Silencing of *GhB9SHZ1* or *GhGT2* interferes with CesA-mediated cellulose biosynthesis and reduces fiber cell wall thickness. A, RT–qPCR analysis of relative *GhB9SHZ1* and *GhGT2* transcript levels in fibers from the WT, a vector control plant and three independent lines for

(continued)

domain of each gene into a cotton leaf crumple virus (CLCrV) vector, and infiltrated cotton plants with Agrobacterium harboring these CLCrV vectors. For each TF, we selected three independent VIGS lines exhibiting significantly lower transcript levels for phenotypic analysis (Figure 6A). RT–qPCR results indicated that the expression levels of *CesA8* and *CesA7-2* genes in *GhB9SHZ1*-silenced plants injected with *pCLCrV:GhB9SHZ1*, as well as*CesA7-1* gene expression in *GhGT2*-silenced plants injected with *pCLCrV:GhGT2*, were significantly lower (Figure 6B). Along with the decreased expression of the *CesA* genes, the fiber cells from cotton lines injected with *pCLCrV:GhB9SHZ1* or *pCLCrV:GhGT2* showed significantly decreased cell wall thickness and less cellulose accumulation compared to the WT and vector control plants (Figure 6, C–H; Supplemental Figure S25). These results confirmed that GhB9SHZ1 and GhGT2, the expression of whose encoding genes is induced by SLs, positively regulate their downstream gene *CesA* expression to modulate cellulose-dependent cell wall thickness.

Similarly, using the same method as above, we generated two sets of silenced cotton plants with significantly lower transcript levels for *GhBLH51* or *NAC100-2* compared to the WT and vector control plants (Figure 7A). Individually silencing the three TF genes (*GhBLH51*, *GhGT2*, and *GhNAC100-2*) that encoded proteins capable of binding to the *KCS5* and *KCS23* promoters resulted in significantly lower expression of the two *KCS* genes, leading to shorter fibers compared to the WT and vector control plants (Figure 7, B and C; Supplemental Figure S26).

Remarkably, compared to the WT and vector control plants, the content of VLCFA up to C26:0 was significantly reduced but that of C24:0 increased in *GhBLH51*-silenced plants injected with *pCLCrV:GhBLH51*, which experienced lower *KCS5* transcript levels (Figure 7D). Moreover, we detected significantly lower C22:0 along with much higher C20:0 contents in *GhGT2*-silenced plants injected with *pCLCrV: GhGT2*, alongside decreased relative *KCS23* expression (Figure 7E). These results suggest that KCS5 and KCS23 are responsible for the conversion of C24:0 to C26:0 and of C20:0 to C22:0, respectively. Congruently, in the *GhNAC100-2*-silenced plants injected with *pCLCrV: GhNAC100-2* that showed lower expression for both *KCS5* and *KCS23*, the contents of C22:0 and C26:0 simultaneously decreased along with the increased accumulation of C20:0 and C24:0 (Figure 7F).

Taken together, *in planta* experiments showed that GhB9SHZ1, GhBLH51, GhGT2, and GhNAC100-2 mediate the SL signal, and are responsible for transmitting the SL signal to their downstream genes, *KCS* and *CesA*, to modulate VLCFA and cellulose biosynthesis and thus fiber cell elongation and cell wall thickness.

Functional characterization of the two *KCS* genes regulated by SL-inducible TFs

In the above VIGS experiments, the *KCS5* and *KCS23* genes regulated by SL-inducible TFs displayed functional differences in VLCFA biosynthesis. To characterize their function in more detail, we performed a genetic complementation assay using the yeast (*Saccharomyces cerevisiae*) *elo2 elo3* double mutant (*Δelo2Δelo3*). Yeast Elo2p is responsible for elongation of fatty acids up to C24, while Elo3p is essential for the conversion of C24–C26 (Toke and Martin, 1996). Yeast cells with both *ELO2* and *ELO3* genes deleted are synthetically lethal (Oh et al., 1997). We determined that expressing either cotton *KCS5* or *KCS23* gene into the double mutant background rescued its lethality phenotype (Figure 8A). Consistently, the *Δelo2Δelo3* mutant carrying cotton *KCS5* or *KCS23* displayed an almost WT growth rate as observed on yeast extract, peptone, dextrose (YPD) solid plates (Figure 8B) and in YPD liquid medium by continuous culture (Figure 8C).

Additionally, *Δelo2Δelo3* yeast cells expressing cotton *KCS5* showed almost identical VLCFA profiles to those of WT cells (Figure 8D), suggesting that KCS5 contributes to the biosynthesis of VLCFAs up to C26:0. Notably, *Δelo2Δelo3* yeast cells expressing *KCS23* showed an accumulation of C22:0, with drastically reduced C24:0 and undetectable levels of C26:0 (Figure 8D), indicating that KCS23 is mainly responsible for the synthesis of C22:0 from C20:0 fatty acids. These results verified the functional differences between KCS23 and KCS5 in VLCFA biosynthesis.

GA enhances SL biosynthesis to promote fiber cell elongation and cell wall thickness

Our above results showed that SL promotes cotton fiber elongation and cell wall thickness, similar to the effect of GA previously reported on cotton fiber development (Shan et al., 2014; Xiao et al., 2016). Based on these findings, we explored the regulatory topology of GA- and SL-dependent coordination of cotton fiber elongation and cell wall thickness.

Figure 6 (Continued)
GhB9SHZ1 or *GhGT2* silenced plants. B, Relative expression levels of *GhCesA8*, *GhCesA7-1*, and *GhCesA7-2* in fibers from *GhB9SHZ1*/*GhGT2*-silenced or nonsilenced cotton plants shown in (A). C, Cross-sections of paraffin-embedded 25-DPA fibers from *GhB9SHZ1*-silenced or nonsilenced cotton plants shown in (A), which were stained with S4B (top) or calcofluor white (bottom). Scale bars, 20 μm. D, Mean cell wall thickness of fibers from *GhB9SHZ1*-silenced or nonsilenced cotton plants shown in (A). Thirty fibers from three ovules were used for each sample, and each fiber was measured 3 times. E, Mean cellulose content of fibers from *GhB9SHZ1*-silenced or nonsilenced cotton plants shown in (A). F, Cross-sections of paraffin-embedded 25-DPA fibers from *GhGT2*-silenced or nonsilenced cotton plants were stained with S4B (top) or calcofluor white (bottom). Scale bars, 20 μm. G, Mean cell wall thickness of fibers from *GhGT2*-silenced or nonsilenced cotton plants shown in (A). Thirty fibers from three ovules were used for each sample, and each fiber was measured 3 times. H, Mean cellulose content of fibers from *GhGT2*-silenced or nonsilenced cotton plants shown in (A).Mean are means ± SD from three independent experiments. Statistical significance was determined using one-way ANOVA combined with Tukey's test. $^{*}P < 0.05$; $^{**}P < 0.01$; $^{***}P < 0.001$.

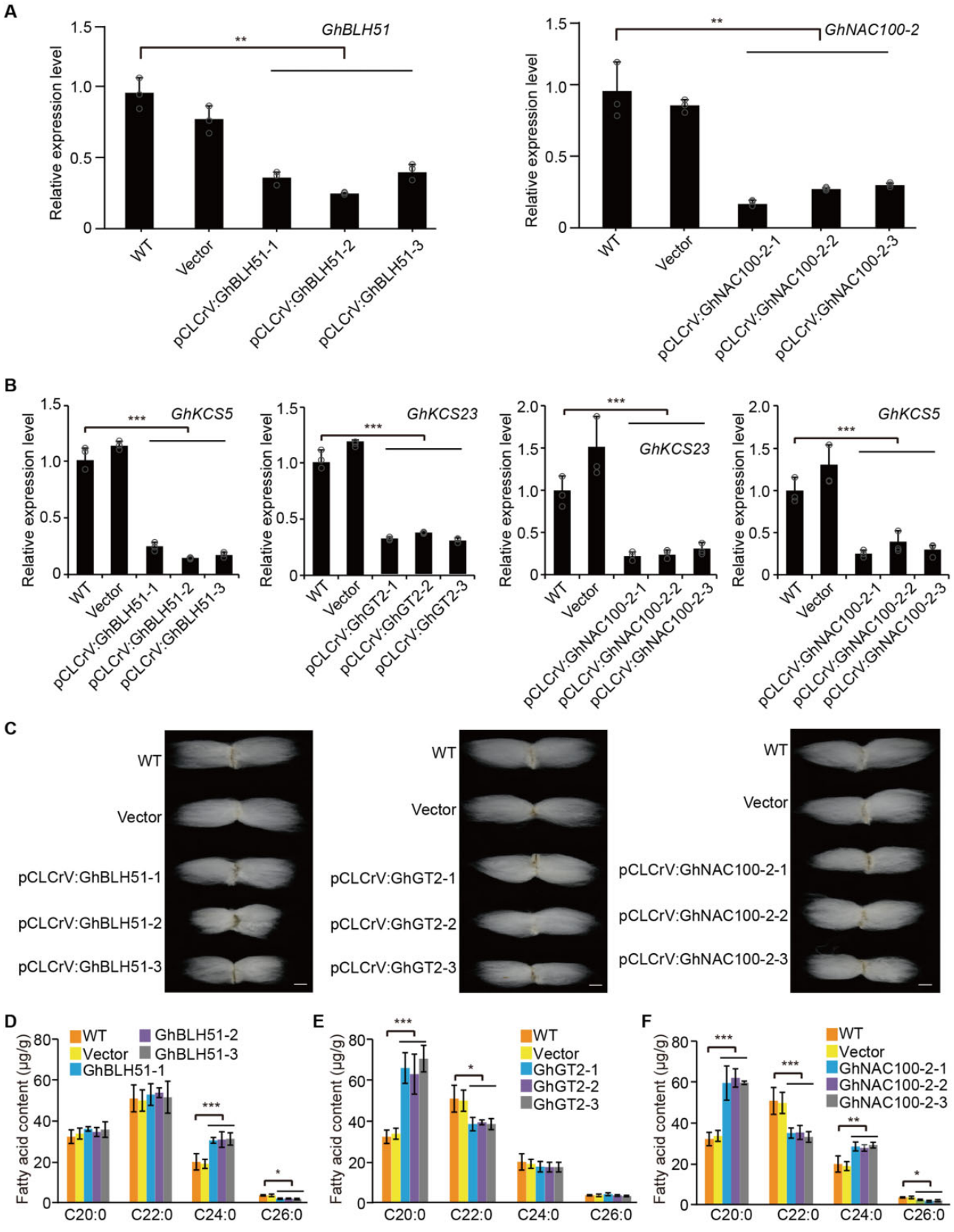

Figure 7 Silencing of *GhBLH51*, *GhNAC100-2* or *GhGT2* interferes with KCS-mediated VLCFA biosynthesis in cotton and inhibits fiber cell elongation. A, RT–qPCR analysis of *GhBLH51* and *GhNAC100-2* relative transcript levels in fibers from WT, a vector control plant and three independent lines of *GhBLH51-* or *GhNAC100-2*-silenced plants. B, Relative expression levels of *GhKCS5* and *GhKCS23* in fibers from *GhBLH51-*, *GhNAC100-2-*, or *GhGT2*-silenced or nonsilenced cotton plants shown in (A) and Figure 6A. C, Analysis of fiber length from nonsilenced cotton plants or *GhBLH51-*,

(continued)

First, co-treatment with GR24 and the GA biosynthesis inhibitor PAC demonstrated that GR24 treatment reverses the inhibitory effect of PAC on cotton fiber development, while GA_3 failed to reverse the inhibitory effect of the SL biosynthesis inhibitor Tis108 (Figure 9A; Supplemental Figure S27). These results suggest that SL-dependent fiber cell elongation and cell wall thickness occur downstream of the GA signaling cascade.

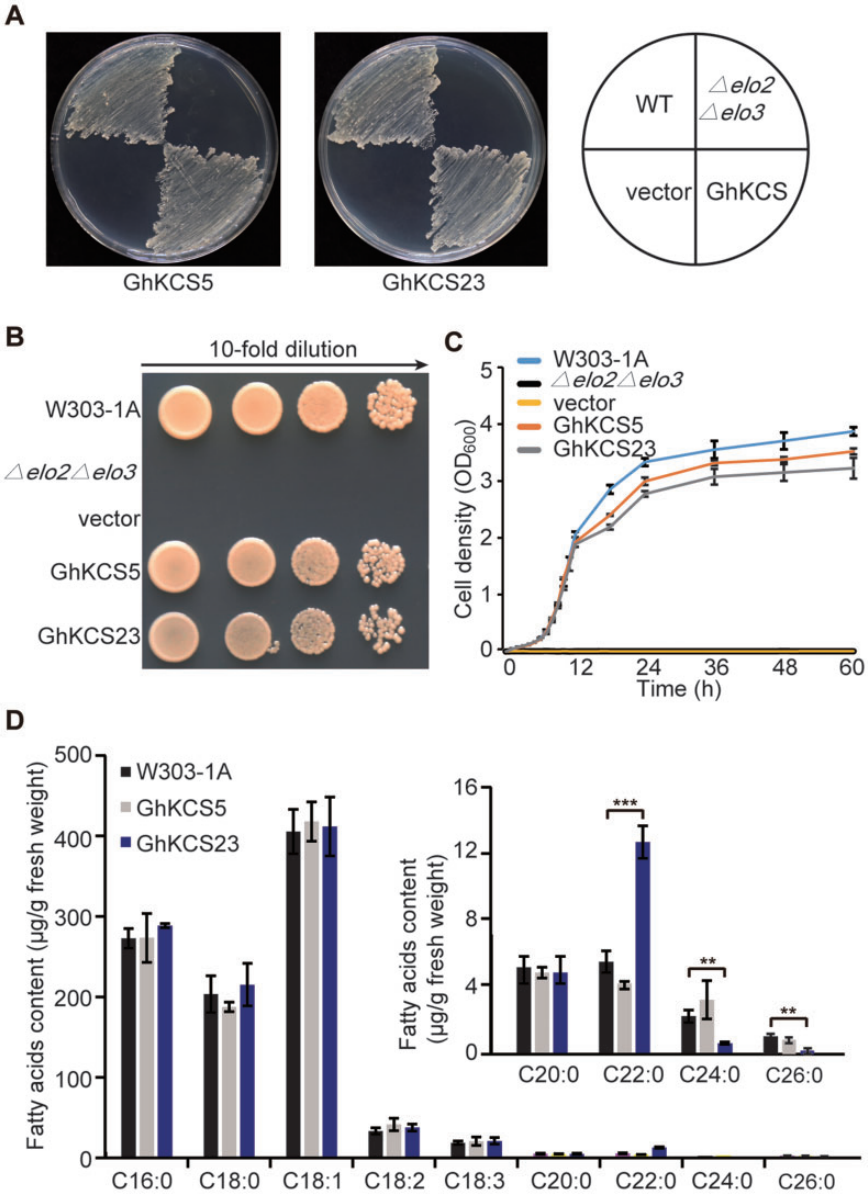

Figure 8 Cotton *GhKCS5* and *GhKCS23* genes rescue the lethal phenotype of the yeast Δ*elo2*Δ*elo3* double mutant. A, Expression of the cotton genes *GhKCS5* or *GhKCS23* rescues the growth ability of the yeast synthetic-lethal Δ*elo2*Δ*elo3* double mutant. B and C, Detailed growth performance analysis of the Δ*elo2*Δ*elo3* double mutant yeast cell lines expressing *GhKCS5* or *GhKCS23* and the WT strain W303-1A. Ten-fold dilution series showing the density of the colonies expressing *GhKCS5* or *GhKCS23* (B). Growth curves of the same yeast strains (C). D, VLCFA contents in WT yeast cells or the Δ*elo2*Δ*elo3* double mutant expressing *GhKCS5* or *GhKCS23*. Data are means ± SD from three independent experiments. Statistical significance was determined by using one-way ANOVA combined with Tukey's test. $^{**}P < 0.01$; $^{***}P < 0.001$. WT yeast strain W301-1A used for genetic transformations.

Figure 7 (Continued)
GhNAC100-2-, and *GhGT2*-silenced cotton plants shown in (A) and Figure 6A. Scale bars, 1 cm. D, VLCFA contents in 10-DPA fibers from nonsilenced cotton plants or *GhBLH51*-silenced cotton plants shown in (A). E, VLCFA contents in 10-DPA fibers from nonsilenced cotton plants or *GhGT2*-silenced cotton plants shown in Figure 6A. F, VLCFA contents in 10-DPA fibers from nonsilenced cotton plants or *GhNAC100-2*-silenced cotton plants shown in (A). Data are means ± SD from three independent experiments. Statistical significance was determined using one-way ANOVA combined with Tukey's test. $^{*}P < 0.05$; $^{**}P < 0.01$; $^{***}P < 0.001$.

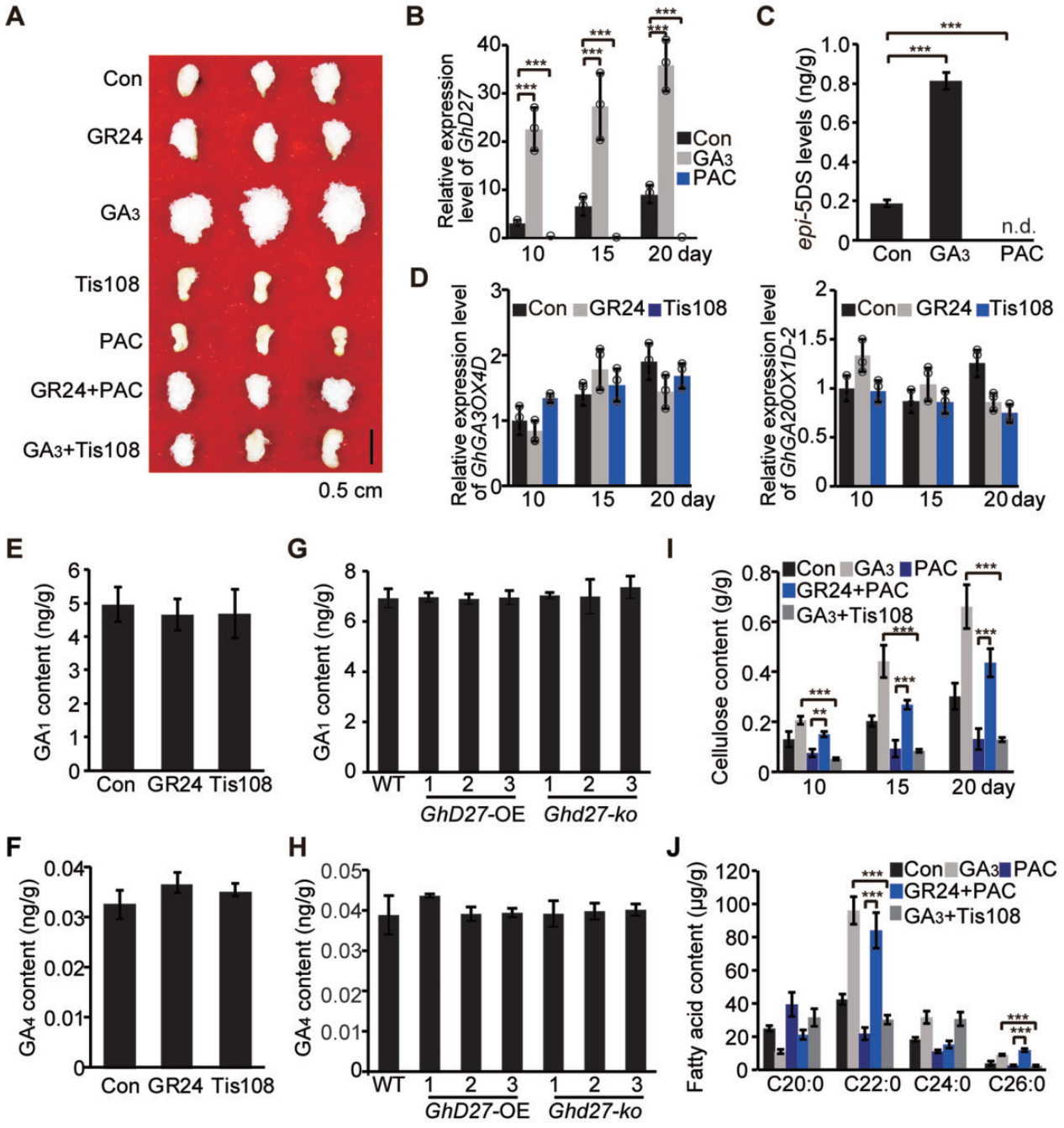

Figure 9 SLs act downstream of GA signaling to regulate fiber cell elongation and cell wall thickness. A, Phenotypes of fibers (collected at 1 DPA) cultured in vitro with 15-μM GR24, 10-μM Tis108, 1-μM GA_3, 5-μM PAC (GA biosynthesis inhibitor), 15-μM GR24 + 5-μM PAC, or 1-μM GA_3 +10-μM Tis108 for 10 days. Scale bar, 5 mm. B, Relative expression levels of *GhD27* after treatment of fibers with 1-μM GA_3 or 5-μM PAC for 10, 15, or 20 days. C, *epi*-5DS contents in untreated fibers and fibers treated with 1-μM GA_3 or 5-μM PAC for 10 days. D, Relative expression levels of *GA3OX4D* (left) and *GA20OX1D-2* (right) in fibers treated with 15-μM GR24 or 10-μM Tis108 for 10, 15, or 20 days. E, GA_1 contents in fibers after treatment with 15-μM GR24 or 10-μM Tis108 for 10 days. F, GA_4 contents in fibers after treatment with 15-μM GR24 or 10-μM Tis108 for 10 days. G, GA_1 contents of cotton fibers from the WT, *GhD27*-OE, and *Ghd27-ko*. H, GA_4 contents of cotton fibers from the WT, *GhD27*-OE, and *Ghd27-ko*. I, Cellulose contents in fibers treated with 1-μM GA_3, 5-μM PAC, 15-μM GR24 + 5-μM PAC, or 1-μM GA_3 + 10-μM Tis108 for 10, 15, or 20 days. J, VLCFA (C20:0, C22:0, C24:0, and C26:0) contents in fibers after treatment with 1-μM GA_3, 5-μM PAC, 15-μM GR24 + 5-μM PAC, or 1-μM GA_3 + 10-μM Tis108 for 10 days. Data are means ± SD (n = 12–25). Statistical significance was determined using one-way ANOVA combined with Tukey's test. $^{***}P < 0.001$. Con, untreated fibers.

To investigate whether GA regulates fiber cell elongation solely through the SL pathway or via other pathways, we treated the *Ghd27-ko* line with GA_3 or *GhD27*-OE with PAC. We observed that the application of GA_3 significantly increases the length of fibers from the *Ghd27-ko* line, but its fibers were still shorter than WT cotton fibers treated with

GA_3 (Supplemental Figure S28A). Conversely, the treatment of *GhD27*-OE transgenic cotton with PAC prominently decreased fiber length, together with cellulose and VLCFA contents, although fibers were much longer than those from PAC-treated WT cotton (Supplemental Figure S28). These results suggest that in addition to the SL pathway, there might be other signaling pathways involved in GA-promoted fiber elongation.

Moreover, RT–qPCR analysis of SL biosynthesis-related genes showed that GA_3 treatment significantly increases the expression of *GhD27*, *GhMAX1*, *and GhMAX3* (Figure 9B; Supplemental Figure S29), resulting in an increase in *epi*-5DS content in the fibers (Figure 9C). In contrast, PAC treatment downregulated the expression of *D27* together with a concomitant decrease of *epi*-5DS levels in the fibers (Figure 9, B and C). Treatment with either GR24 or Tis108 did not significantly alter the expression levels of *GA 20-oxidase1D-2* (*GA20OX1D-2*) or *GA 3-oxidase4D* (*GA3OX4D*), encoding two key enzymes participating in GA biosynthesis (Figure 9D). Accordingly, contents of the two main active GAs (GA_1 and GA_4) in fibers treated with GR24 or Tis108 were comparable to those in untreated fibers (Figure 9, E and F). Likewise, contents of GA_1 and GA_4 in fibers of *GhD27* overexpressing or knockout lines were comparable to those in fibers of WT plants (Figure 9, G and H). These results suggest that the SL pathway is downstream of the GA signaling cascade and that GA regulates D27-mediated SL biosynthesis. Additionally, we demonstrated that increased biosynthesis of cellulose and VLCFAs in fiber cells resulting from GA treatment is abolished by the SL biosynthesis inhibitor Tis108 (Figure 9, I and J). Conversely, the suppression of cellulose and VLCFA biosynthesis by the GA biosynthesis inhibitor PAC was rescued by GR24 treatment (Figure 9, I and J). These results further support the view that SL signaling acts downstream of the GA pathway. Taken together, we propose that GA promotes D27-mediated SL biosynthesis to enhance VLCFA and cellulose biosynthesis in cotton fiber cells.

Knocking out of *GhGRF4* interferes with SL-mediated fiber cell elongation and cell wall thickness

To explore the potential mechanisms by which D27-mediated SL biosynthesis is modulated by GA, we performed another RNA-seq analysis using three sets of transcriptomes obtained from untreated cotton fibers, fibers treated with GA, and fibers treated with PAC. We looked for those TF genes whose expression was upregulated by GA but downregulated by PAC treatment (Supplemental Table S3), yielding 15 candidate TF genes. Systematic Y1H assays revealed that among the 15 TFs, only GhGRF4 specifically binds to the *GhD27* promoter (Figure 10A; Supplemental Figure S30). The *GRF* family in *G. hirsutum* comprises 33 *GhGRF* genes, with *GhGRF4* (Gh_D09G1332) used in this study being highly expressed in 25-DPA fibers and 0-DPA ovules, roots, and pistils (Supplemental Figure S31). RT–qPCR analysis showed that the expression of *GhGRF4* is significantly upregulated by GA_3 treatment (Supplemental Figure S32). LUC reporter assays further revealed the binding and transcriptional activity of GhGRF4 on the *D27* promoter (Figure 10, B and C). To identify the exact binding site of GhGRF4 on the *D27* promoter, we performed a bioinformatics analysis that identified two potential GRF-binding sites (Figure 10D; Supplemental Figure S33). Y1H and LUC reporter assays demonstrated that GhGRF4 specifically binds to the first GRF-binding site rather than the second to activate *GhD27* transcription (Figure 10, E–G). EMSA showed that recombinant GhGRF4 exhibits binding affinity for *GhD27* promoter fragments containing the GRF binding site (Figure 10H). This affinity was reduced by adding increasing amounts of unlabeled intact probes but was not affected by adding increasing amounts of unlabeled mutated probes (Figure 10I). These results confirmed the specific binding activity of GhGRF4 to the *GhD27* promoter via the GRF-binding site.

Taking these results together, we propose that GA induces the expression of *GhGRF4*, whose encoding TF directly activates the transcription of the key SL-biosynthesis gene *GhD27* to strengthen SL-mediated cotton fiber cell elongation and cell wall thickness.

To further confirm that GA-inducible GhGRF4 is crucial for activating SL biosynthesis and SL-mediated cell elongation and cell wall thickness, we developed cotton mutant lines in which *GhGRF4* had been knocked (*Ghgrf4-ko*) via CRISPR/Cas9-mediated genome editing (Supplemental Figure S34). We selected three independent *Ghgrf4-ko* lines, in which the function of GRF4 was abolished without affecting the transcription of its encoding gene for experimental analysis (Supplemental Figure S35). RT–qPCR showed that knocking out *GhGRF4* significantly inhibits the expression of the SL biosynthetic gene *GhD27* and resulted in a pronounced decrease in *epi-5DS* content (Figure 10, J and K). Accordingly, the *Ghgrf4-ko* transgenic line exhibited dramatically shortened cotton fibers and decreased cell wall thickness compared to WT (Figure 10, L–O; Supplemental Figure S36). These results indicated that knocking out the GA-inducible *GhGRF4* interferes with SL biosynthesis and thus impedes SL function in fiber cell elongation and cell wall thickness.

Furthermore, we investigated the expression levels of genes downstream of the SL signaling pathway in the *Ghgrf4-ko* line, including the four SL-inducible TF genes (*GhNAC100-2*, *GhBLH51*, *GhGT2*, and *GhB9SHZ1*), and the TF-regulated genes related to cellulose biosynthesis (*GhCesA8*, *GhCesA7-2*, and *GhCesA7-1*) and VLCFA biosynthesis (*GhKCS5* and *GhKCS23*). RT–qPCR analysis demonstrated that knocking out *GhGRF4* leads to the significantly lower expression of these genes downstream of the SL signal (Figure 10, P–R). Accordingly, in comparison to the WT, cellulose and VLCFA (C22:0 and C26:0) contents were prominently decreased in fiber cells from *Ghgrf4-ko* plants as well (Figure 10, S and T), resulting in its decreased cell wall thickness and shortened cotton fibers (Figure 10, L–O).

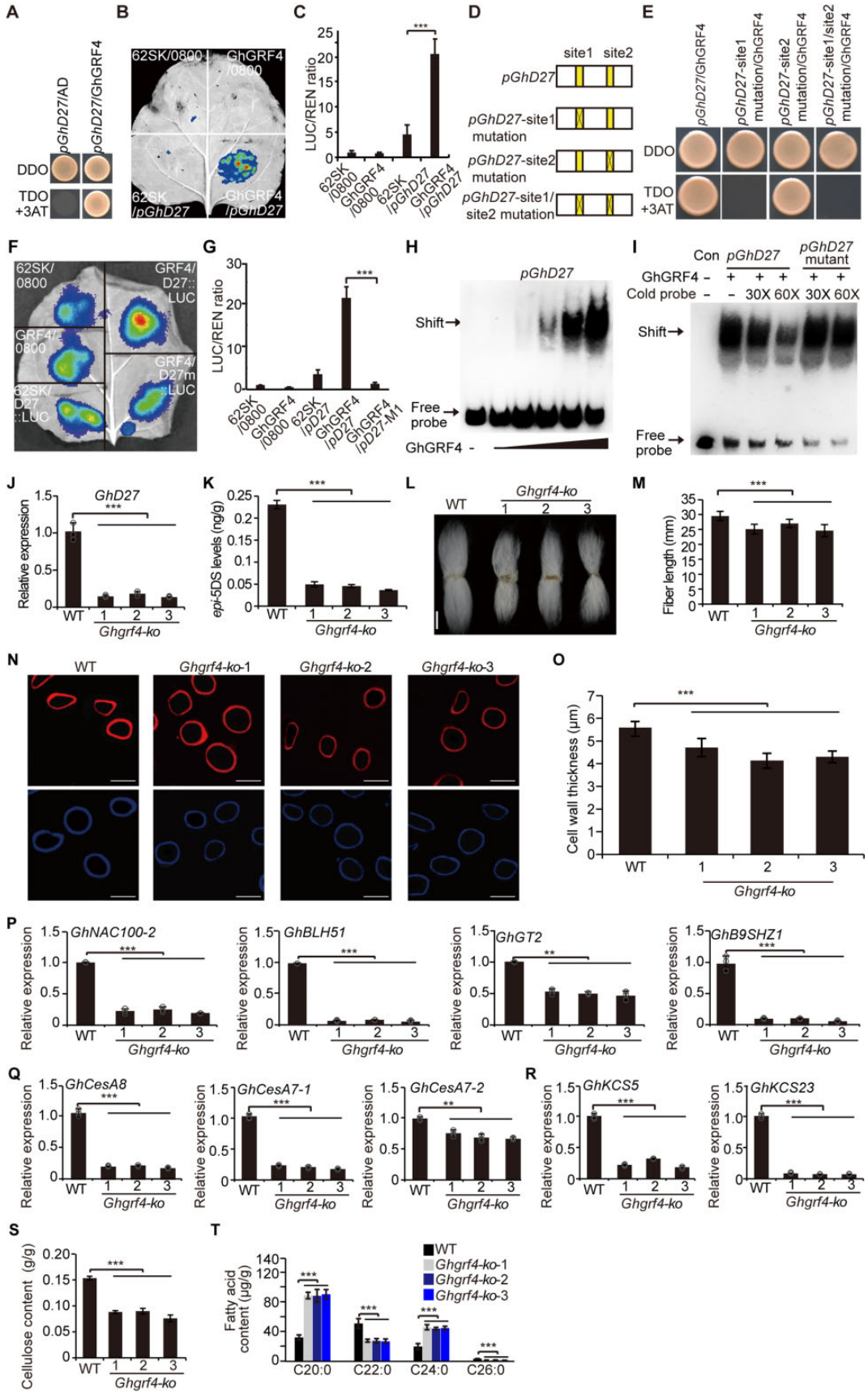

Figure 10 Knocking out the GA-inducible TF gene, *GhGRF4*, interferes with the effect of GA on SL-mediated fiber cell elongation and cell wall thickness. A, Y1H assay showing the binding of GhGRF4 to the *GhD27* promoter. B, Transient expression assay in *N. benthamiana* leaves showing

(continued)

Taken together, knocking out *GhGRF4* inhibits SL biosynthesis and interferes with the SL signaling pathway involved in fiber cell elongation and cell wall thickness, suggesting that GhGRF4 acts as the bridge to link the crosstalk between GA and SL. These findings further support our view that SLs act downstream of GA signaling in regulating the cell elongation and cell wall thickness that shape fiber cell length and strength.

Discussion

Harnessing the GA–SL crosstalk signal to improve fiber quality via simultaneously promoting fiber cell length and cell wall thickness

The economic value of cotton fibers is largely dependent on fiber length, the most important trait determined by fiber cell elongation and cell wall thickness (Kim and Triplett, 2001; Tausif et al., 2018). VLCFAs, whose biosynthesis is catalyzed by KCS proteins, are essential in fiber cell elongation (Qin et al., 2007). It has been reported that the two phytohormones, GA and ethylene, are implicated in VLCFA-mediated fiber cell elongation (Shi et al., 2006). GA promotes the expression of *KCS* genes to enhance VLCFA biosynthesis in fiber cells, indicating that VLCFAs are downstream of GA signaling in fiber cell elongation (Xiao et al., 2016). However, VLCFAs act upstream of ethylene, because applying VLCFA promotes ethylene biosynthesis in cotton fiber cells (Qin et al., 2007). The regulatory machinery of the GA–VLCFA–ethylene module in fiber cell elongation has therefore remained elusive. Here, we showed that the other plant hormone, SL, is implicated in the GA–VLCFA–ethylene module, suggesting crosstalk of three phytohormones in the regulation of fiber cell elongation.

We demonstrated that SLs mediate the transmission of the GA signal to VLCFA biosynthesis (Figure 11). Genetic, biochemical, transcriptomic, and gene expression lines of evidence identified several components involved in this hierarchical regulatory pathway: (1) GhGRF4, the top-layer (upstream) TF whose encoding gene is induced by GA, directly activates transcription of the SL biosynthetic gene *D27*, leading to much higher SL accumulation and (2) The accumulated SLs induce the expression of three second-layer TF genes (*GhNAC100-2*, *GhBLH51*, and *GhGT2*), whose encoded TFs directly activate the transcription of their downstream genes, *KCS5* and *KCS23*, to enhance the biosynthesis of VLCFAs. The complete signaling cascade we revealed is responsible for modulating fiber cell elongation.

Cellulose is crucial for cell wall thickness and plant mechanical strength (Zhong et al., 2019). In this study, we showed that in addition to regulating cell elongation, the GA–SL crosstalk also regulates cellulose biosynthesis to modulate cell wall thickness. Moreover, we identified several TFs involved in this level of the GA–SL module: (1) The first step of GA signaling transduction relies on the top-layer TF GhGRF4, which transmits the GA signal downstream to SL biosynthesis (Figure 11). Moreover, *GRF* gene family members were reported to be closely associated with the transmission of GA signaling (Lantzouni et al., 2020). In *G. hirsutum*, we identified 33 *GhGRF* genes in total (Supplemental Figure S31), some of which were highly expressed in fiber cells. These results strongly suggest that in addition to *GhGRF4*, other *GhGRF* members may be involved in mediating the GA signal related to fiber development as well. (2) Then, accumulated SLs induce the expression of *GhGT2* and *GhB9SHZ1*, the second-layer TF genes, whose encoded proteins directly bind to the promoters of their downstream genes *CesA7-1*, *CesA7-2*, and *CesA8* to activate their transcription and therefore enhance cell wall thickness.

Taken together, in this study, we show the possibility of promoting fiber cell length together with cell wall thickness by harnessing the GA–SL module, offering a path to

Figure 10 (Continued)
the transcriptional activation of the *LUC* reporter gene (driven by the *GhD27* promoter) by the TF GhGRF4. C, Quantification of LUC activity in (B). *Renilla* (REN) activity was used for normalization. The LUC/REN ratio indicates the relative activity of the promoter. D, Identification of two potential GRF-binding sites in the *GhD27* promoter. E, Y1H assays showing the binding of GhGRF4 to the first but not the second putative GRF-binding site in the *GhD27* promoter. F, Transient expression assay to evaluate the transcriptional activity of the *LUC* reporter gene driven by the intact *GhD27* promoter or the *GhD27* promoter with the GRF-binding site(s) mutated. G, Quantification of the LUC activity in (F). REN activity was used for normalization. The LUC/REN ratio indicates the relative activity of the promoter. H, EMSA showing that GhGRF4 binds directly to the *GhD27* promoter fragment containing GRF-binding sites. The biotin-labeled DNA fragment from the *GhD27* promoter containing the intact GRF-binding sites were incubated with increasing amounts of maltose-binding protein (MBP)-GhGRF4. I, Competition of binding between biotin-labeled DNA fragments and MBP-GhGRF4 by different concentrations of the cold probes (without biotin-labeling) with intact or mutated GRF-binding sites. J, RT–qPCR analysis of relative *GhD27* transcript levels in fibers from WT and *GhGRF4*-knockout lines (*Ghgrf4-ko*). K, *epi*-5DS contents of 10-DPA cotton fibers collected from the WT and three independent *Ghgrf4-ko* lines. L, Representative images of mature fibers from WT and *Ghgrf4-ko* transgenic plants. Scale bar, 1 cm. M, Length of mature fibers from WT and *Ghgrf4-ko* transgenic plants. N, Cross-sections of paraffin-embedded 25-DPA fibers from WT and *Ghgrf4-ko* lines that were stained with S4B (top) or calcofluor white (bottom). Bars = 20 μm. O, Mean cell wall thickness of fibers from WT and *Ghgrf4-ko* cotton plants. Thirty fibers from three ovules were used for each sample, and each fiber was measured 3 times. P, Relative expression levels of SL-inducible TF genes (*GhNAC100-2*, *GhBLH51*, *GhGT2*, and *GhB9SHZ1*) in fibers from WT and *Ghgrf4-ko* cotton plants. Q, RT–qPCR analysis of relative expression levels of *GhCesA8*, *GhCesA7-2*, and *GhCesA7-1* in fibers from WT and *Ghgrf4-ko* cotton plants. R, Relative expression levels of *GhKCS5* and *GhKCS23* in fibers from WT and *Ghgrf4-ko* cotton plants. S, Cellulose content of fibers from WT and *Ghgrf4-ko* cotton plants. T, VLCFA contents in 10-DPA fibers from WT and *Ghgrf4-ko* cotton plants. Data are means ± SD from three independent experiments. Statistical significance was determined using one-way ANOVA combined with Tukey's test. ***$P < 0.001$. WT (jin668).

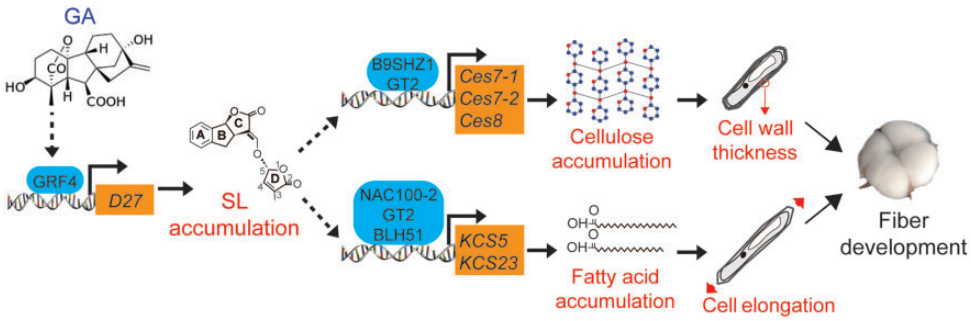

Figure 11 Schematic diagram depicting the mechanistic framework of SL-GA crosstalk signaling in the regulation of cotton fiber cell elongation and cell wall thickness.

combining multiple advantageous traits of cotton fibers and thus improving their quality.

SL enhances cell wall thickness without penalties on cell elongation

There is typically a tradeoff between fiber cell elongation and secondary cell wall thickness (Gou et al., 2007; Niu et al., 2019; Cao et al., 2020), based on observations that many identified genes or components promoting fiber cell elongation usually attenuate cell wall thickness, and vice versa. Generally, secondary cell wall thickening by cellulose deposition promotes plant cell strength at the expense of gradual loss of its extensibility and incorporative ability, leading to inhibited cell elongation (Cosgrove and Jarvis, 2012; Anderson and Kieber, 2020). Nevertheless, in this study, we showed that SL not only promotes cell elongation but also enhances secondary cell wall thickness. These results suggest that in addition to advancing CesA-mediated cellulose accumulation, SL is highly likely to regulate other components associated with the secondary cell wall, which confers the extension or stretch ability to the secondary cell wall and thus facilitates cell expansion for elongation. Consistent with the above hypothesis, secondary cell wall has been reported to undergo various deformation processes under some conditions that resemble, to some degree, primary cell wall growth (Houston et al., 2016; Anderson and Kieber, 2020; Gigli-Bisceglia et al., 2020). This deformation occurs through modifying the composition of the cell wall or by regulating cell wall-associated proteins, such as expansins that induce stress relaxation and sustained creep of cell walls (Sampedro and Cosgrove, 2005; Gigli-Bisceglia et al., 2020). Therefore, uncovering the potential components involved in SL-mediated extension of the secondary cell wall will provide insights into understanding the mechanism underlying the mechanical dynamics of the secondary cell wall.

Crosstalk between SLs and GA is ubiquitous but its regulatory machinery differs in flowering plants

SLs elicit their control on plant morphology and physiology via direct or indirect interaction with other plant hormones (Duan et al., 2019). The interaction/crosstalk between SLs and phytohormones such as auxin, cytokinin, and ethylene has been extensively studied in Arabidopsis and rice (*Oryza sativa*) (Agusti et al., 2011; Zhang et al., 2020). However, evidence regarding the SL–GA crosstalk is minimal and only from rice. In rice, D14, an essential component of plant SL signaling, interacts with the GA signaling repressor SLR1 (Nakamura et al., 2013). Furthermore, GA is capable of regulating SL biosynthesis in rice to control parasitic weed infections (Ito et al., 2017). Combined with our findings (Figure 11), the existence of GA–SL crosstalk in both monocot (rice) and dicot (cotton) plants suggests that this phytohormonal crosstalk is probably ubiquitously present in flowering plants to regulate their development and fitness.

Notably, GA inhibits SL biosynthesis to prevent parasitic weed infections in rice (Ito et al., 2017). In contrast, GA promotes SL biosynthesis to enhance cotton fiber cell elongation and cell wall thickness (Figure 11). The disparate regulatory models of SL biosynthesis by GA indicate that the GA–SL phytohormonal crosstalk is varied in the regulation of different biological processes in different plant species. In the future, unveiling the interplay between GA and SLs in the development of more plant species would be helpful to further understand the mechanistic complexity of GA–SL crosstalk.

The role of GA–SL crosstalk in development of other plant single-cell models

The function of SLs in the development of whole plant body organization or individual organs has been established, yet how SLs control the behavior of single cells is still unknown. Generally, three classic single-cell models have been used in studies of plant cell patterning and development: (1) root hairs, a model for studying cell elongation, tip growth, cell wall modifications (Hossain et al., 2015); (2) trichomes, namely plant leaf hairs, serving as a single-cell model to study plant cell differentiation and cell patterning (Hülskamp, 2004; Yang and Ye, 2013); and (3) cotton fiber cells, a model for studying cell elongation and cell wall biosynthesis (Kim and Triplett, 2001; Huang et al., 2021).

Most studies regarding SL-mediated plant cell development tend to focus on root hair development. Additionally, development of the three single-cell models displayed partial regulatory conservation, because they often recruit the same

components/genes to regulate similar biological processes, as exemplified by ethylene and VLCFAs promoting both cotton fiber and Arabidopsis root hair growth by activating pectin biosynthesis (Pang et al., 2010). Therefore, the knowledge we gained from studying GA–SL crosstalk in fiber cell provides an insight into revealing the regulatory mechanism underlying the development of two other single-cell models—root hairs and trichomes—and also enriches our understanding of the SLs in plant development at the single-cell level.

Materials and methods

Plant materials and in vitro ovule culture

The Upland cotton (*G. hirsutum*) cultivar "Xuzhou-142," "jin668," and *GhD27* transgenic plants were grown in a greenhouse with 60% humidity, a 16-h light/8-h dark cycle, and a temperature of 30°C. The lighting was provided by a LED flat panel with an intensity of 80,000 lux. Cotton bolls were harvested at 0, +5, +10, +15, and +20 DPA from WT and transgenic plants. Fibers and ovules at 0 to +20 DPA were harvested and stored at −80°C before use.

For the GR24, GA_3, Tis108, and PAC treatments, ovules were harvested at +1 DPA, surface-sterilized in 10% (w/v) sodium hypochlorite solution, and independently cultured with 15-μM GR24, 10-μM Tis108, 0.5-μM GA_3, or 5-μM PAC at 30°C under aseptic conditions. The composition of the culture medium was as follows: 6.183-mg L^{-1} H_3BO_3, 272.18-mg L^{-1} KH_2PO_4, 441.06-mg L^{-1} $CaCl_2{\cdot}2H_2O$, 0.024-mg L^{-1} $CoCl_2{\cdot}6H_2O$, 0.242-mg L^{-1} $Na_2MoO_4{\cdot}2H_2O$, 0.83-mg L^{-1} KI, 16.902-mg L^{-1} $MnSO_4{\cdot}H_2O$, 493-mg L^{-1} $MgSO_4{\cdot}7H_2O$, 8.627-mg L^{-1} $ZnSO_4{\cdot}7H_2O$, 5,055.5-mg L^{-1} KNO_3, 0.025-mg L^{-1} $CuSO_4{\cdot}5H_2O$, 11.167-mg L^{-1} Na_2EDTA, 8.341-mg L^{-1} $FeSO_4{\cdot}7H_2O$, 0.822-mg L^{-1} pyridoxine·HCL (vitamin B6), 0.492-mg L^{-1} nicotinic acid (vitamin B3), 1.349-mg L^{-1} thiamine·HCL (vitamin B1), 18,016-mg L^{-1} D-glucose, 180.16-mg L^{-1} myo-inositol, and 3,603.2-mg L^{-1} D-fructose. The pH of the medium was adjusted to 6.0. Cross-sections of fibers were prepared as previously described (Qin et al., 2007). The samples were observed and photographed under a light microscope.

Vector construction and cotton transformation

The coding sequence of *GhD27* was cloned into the pBI121 vector to construct the overexpression vector. Two single-guide RNA (sgRNA) sequences were designed from the *GhD27* and *GhGRF4* sequence for cloning into the CRISPR/Cas9 vector. All primer sequences are listed in Supplemental Data Set 3. The overexpression and CRISPR/Cas9 vectors were transformed into Agrobacterium (*A. tumefaciens*) strain GV3101. Agrobacterium-mediated cotton transformation was performed as previously described (Li et al., 2009). The hypocotyl explants from jin668 were cut from 5-day-old sterile cotton seedlings for Agrobacterium-mediated transformation. Subsequently, the explants were soaked in the Agrobacterium cell suspension for 20 min and transferred to a callus-induction medium, followed by proliferation, embryogenic callus induction, embryo differentiation, and plantlet regeneration. Finally, the putative transgenic plants were transferred to a greenhouse with a 16-h light/8-h dark cycle at 30°C. After selection based on kanamycin resistance and transgene PCR amplification, the T_2 generation of transgenic cotton plants was used for phenotypic analysis. For the *Ghd27-ko* and *Ghgrf4-ko* transgenic cotton, both their genomic DNA and cDNA from D-subgenome were sequenced to confirm the sites edited by the CRISPR/Cas9 system in these knockout lines.

RT–qPCR analysis

Total RNA was extracted from developing cotton fibers using the RNAprep Pure Plant kit (Tiangen, Beijing, China), and 2 μg of total RNA was used for first-strand cDNA synthesis with a Superscript First-Strand Synthesis System (Invitrogen, Carlsbad, CA, USA). Transcript abundance was determined by qPCR assays using SYBR green master mix (2X) (Thermo Fisher Scientific, Foster, CA, USA). The gene-specific primers used in the qPCR experiments are given in Supplemental Data Set 3. The reactions were performed using a Roche Light Cycle 480 II instrument (Roche, Basel, Switzerland) programmed as follows: an initial denaturation at 95°C for 3 min followed by 40 cycles of 95°C for 25 s, 56°C for 30 s, and 72°C for 30 s. A melting curve was generated from 65°C to 95°C with 0.5°C increments. Fluorescence signals were automatically acquired at the end of each cycle. The relative expression levels of the corresponding genes were calculated using the $2^{-\Delta\Delta CT}$ method of Livak and Schmittgen (2001). Three independent biological replicates were performed for each gene.

GA extraction and concentration determination

Ten-day-old fibers were ground thoroughly to a powder in liquid nitrogen. Before the addition of 2 mL 80% (v/v) acetone containing 1% (v/v) acetic acid, the following deuterium-labeled GAs were added as internal standards: D_2-GA_1 (1.00 ng g^{-1}), D_2-GA_4 (2.00 ng g^{-1}). Then, the samples were incubated at 4°C for 12 h and centrifuged at 3,000 *g* for 20 min at 4°C. The supernatants were dried under a stream of nitrogen gas and then dissolved in 1-mL water containing 1% (v/v) acetic acid. For sample purification, the mixture was loaded onto a column (Oasis HLB; Waters) that was washed with one bed volume of water containing 1% (v/v) acetic acid and dried using nitrogen gas. The sample was then dissolved in methanol and transferred to a new column (Bound Elut DEA; Agilent, Santa Clara, CA, USA), washed 2 times with methanol and eluted with 2-mL methanol containing 1% (v/v) acetic acid. Nitrogen gas was used to dry the sample. Finally, the sample was dissolved in 1:1 (v/v) chloroform:ethyl acetate containing 1% (v/v) acetic acid and transferred to a new SepPak silica column (SepPak silica; Waters, Milford, MA, USA), after which it was eluted twice with one bed volume of 1:1 (v/v) chloroform:ethyl

acetate containing 1% (v/v) acetic acid. Following these steps, the GAs were dried under vacuum and dissolved in 200-μL water containing 1% (v/v) acetic acid. An liquid chromatography with tandem mass spectrometry (LC–MS/MS) system consisting of a quadrupole/time-of-flight tandem mass spectrometer (Q Exactive Plus, Thermo Fisher Scientific, Waltham, MA, USA) was used for GA analysis. LC separations and MS/MS conditions were performed as described previously (Kanno et al., 2016).

epi-5DS extraction and quantification

The *epi*-5DS contents were measured as described previously (Jiang et al., 2013).For *epi*-5DS extraction and quantification, 3-g fresh fibers were ground thoroughly to a powder in liquid nitrogen, placed in a tube with 10-mL deionized water, and ultrasonicated with 150 W power and 32–38 kHz for 5 min in an ice water bath after adding 3 ng d_6-5DS as internal standard. An aliquot of 10-mL acetonitrile was then added, and the sample was sonicated again for 10 min and incubated overnight at −20°C. Five gram NaCl was added to the mixture, which was sonicated again for 10 min and then centrifuged at 5,000 *g* for 5 min at 4°C. The supernatant was collected and dried under nitrogen gas in the dark. The pellet was solubilized in 3-mL hexane, dried under nitrogen gas in the dark, and dissolved in 200-μL methanol. The sample was filtered through a 0.22-μm ultrafiltration membrane. The ultraperformance liquid chromatography-tandem mass spectrometry (UPLC–MS/MS) system consisted of a quadrupole/time-of-flight tandem mass spectrometer (Q Exactive Plus, Thermo Fisher) and an Acquity Ultra Performance Liquid Chromatograph (Acquity UPLC; Waters) equipped with a reverse-phase column (SB-C18, 2.1 × 150 mm, 3.5 μm; Agilent). Mobile phase A (99.9% methanol + 0.1% formic acid, v/v) and mobile phase B (99.9% H_2O + 0.1% formic acid, v/v) were pumped at the rate of 0.4 mL min^{-1}. The gradient started with 80% (v/v) A for 5vmin. MS parameters were as follows: desolvation gas flow 800 L h^{-1}, capillary voltage 5 kV, cone voltage 25 V, desolvation temperature 350°C, source temperature 110°C, collision energy 14 V, using multiple reaction monitoring transition of m/z 331 > 217.2 for the *epi*-5DS detection and 337 > 222 for the d_6-5DS detection.

Measurement of cellulose contents

Cellulose extraction and measurement were performed using a cellulose assay kit (Solarbio, China). The fiber samples (300 mg) were frozen in liquid nitrogen and lyophilized, then washed with 0.5-M ice-cold potassium phosphate buffer (0.5 mL, pH 7.0) 3 times. The pellets were washed with deionized water, dispersed in 80% (v/v) ethanol, and incubated at 90°C for 20 min. After cooling to room temperature, the samples were centrifuged at 6,000 *g* for 10 min at room temperature. The pellets were then washed twice, first with 80% (v/v) ethanol and then with acetone. An appropriate amount of deamylase was then added and incubated for 30 min at 37°C to remove starch, the samples were centrifuged at 6,000 *g* for 20 min at room temperature, and the pellets were dried at 50°C. The pellets were dissolved with 72% (v/v) H_2SO_4, and centrifuged for 10 min. The supernatants were then diluted with H_2O and the working solution was added to calculate the cellulose contents by measuring the absorbance at 620 nm.

Fatty acid content measurements

The fatty acid contents were measured as described previously (Qin et al., 2007). Briefly, 10-day-old fibers were immersed in chloroform/methanol (2:1, v/v) for 1 min to remove surface waxes, ground to a powder in liquid nitrogen, and were then extracted 3 times with ethanol:water:diethylether:pyridine:ammonium hydroxide (7.0 N) (15:15:5:1:0.018, v/v). Heptadecanoic acid (C17:0, Sigma-Aldrich, St. Louis, MO, USA) was added to the fatty acid extraction medium to monitor fatty acid recovery and quantification, dried under nitrogen gas, and derivatized by heating to 85°C in H_2SO_4 (3 N) for 5 h. After returning to room temperature, fatty acid methyl esters were extracted 3 times with hexane and then concentrated to a final volume of 200 μL. A GC tandem mass spectrometer (TQ-GC, Xevo) system was used for fatty acid concentration measurement as described previously (Liu et al., 2015).

In vivo dual-LUC assay

For dual-LUC assays, 2,000-bp promoter fragments upstream of *GhCesA8*, *GhCesA7-1*, *GhCesA7-2*, *GhKCS5*, *GhKCS23*, and *GhD27* were amplified from *G. hirsutum* genomic DNA and cloned individually into the pGreenII 0800-LUC vector upstream of the firefly *LUC* reporter gene. The corresponding candidate TF genes were cloned into the pGreenII 62sk vector as the effectors. The primers used are listed in Supplemental Data Set 3. The effector and reporter vectors were transformed into Agrobacterium strain GV3101 and transiently co-infiltrated in *N. benthamiana* leaf epidermis cells. The LUC and REN (*Renilla* LUC) activities were measured via a Dual Luciferase Reporter Assay System kit (Promega Corp., Madison, WI, USA).

RNA-seq data analysis

Total RNA was extracted from 10-day-old fibers treated with GR24, the corresponding inhibitor Tis108, GA_3 and the corresponding inhibitor PAC, or 10-day-old control fibers (CK). An aliquot of 2-μg total RNA per sample was used to construct cotton fiber RNA-seq libraries with an NEB NextUltraTM RNA Library Prep Kit for Illumina (New England Biolabs, Ipswich, MA, USA). An Illumina Hiseq platform (HiSeq 2000) was used to generate 125/150-bp paired-end reads. Three biological replicates were performed for each library. To get high-quality clean reads, the reads were filtered by fastp (version 0.18.0) (Chen et al., 2018), and then mapped against a ribosome RNA (rRNA) database (ftp://ftp.ncbi.nih.gov/genbank) using short reads alignment tool Bowtie2 (version 2.2.8) (Langmead and Salzberg, 2012). The rRNA mapped reads were removed. The paired-end clean reads were mapped to the reference genome (Hu et al., 2019), using HISAT2.2.4 (Kim et al., 2015) with "-rna-

strandness RF" and default parameters. The mapped reads for each sample were assembled with StringTie version 1.3.1 (Pertea et al., 2015). For each transcribed region, the fragment per kilobase of transcript per million mapped reads value was calculated using StringTie software. The differential expression analysis between two groups (GR24 versus CK; GR24 versus Tis108; Tis108 versus CK and GA_3 versus CK; GA_3 versus PAC; PAC versus CK) was performed by DESeq version 2.0 software (Love et al., 2014). The genes with fold-change >2 were identified as DEGs. GO analysis of upregulated genes in each comparison was performed using the Cytoscape version 3.6.1 plug-in ClueGO version 2.5.6 (Bindea et al., 2009). KEGG analysis of genes whose expression was upregulated in each comparison was performed by KOBAS version 3.0 (http://kobas.cbi.pku.edu.cn/).

Y1H assay

For Y1H assays, 2,000-bp promoter fragments from *GhCesA8*, *GhCesA7-1*, *GhCesA7-2*, *GhKCS5*, *GhKCS13*, *GhKCS23*, and*GhD27* were cloned individually into the pHIS2 vector (Clontech, Mountain View, CA, USA). The coding sequences of the candidate TF genes were inserted into the pGADT7 vector (Clontech). The pGADT7 prey vectors carrying the coding sequences of the candidate TF genes and the pHIS2 bait vectors were transformed into the yeast strain Y187. Equal numbers of transformed yeast cells were spotted onto synthetic defined (SD) medium lacking Trp and Leu (DDO), and or Trp, Leu, and His (TDO) with or without 3-mM 3-amino-1,2,4-triazole and incubated at 30°C for 3–5 days.

EMSA

For EMSA, the *GhGRF4*, *GhB9SHZ1*, *GhGT2*, *GhNAC100-2*, and *GhBLH51* coding sequences were individually inserted into the pGEX-6P-1 vector and the recombinant proteins were produced and purified in vitro. The promoter fragment of *D27* containing the intact or mutant GRF-binding site was labeled with biotin on both ends of the probe. The promoter fragment of *CesAs or KCSs* was labeled with biotin on both ends of the probe. Sequences of DNA probes are listed in Supplemental Data Set 3. Unlabeled probes were used as cold competitors. The direct binding activity of proteins to promoter fragments was detected using a LightShift Chemiluminescent EMSA Kit (Thermo Scientific, USA) following the manufacturer's protocol.

Cell wall microscopy analysis

Cotton fibers at 10, 20, 30 DPA and mature fibers were fixed with FAA solution (Ethanol: acetic acid (v:v) = 3:1, containing 1% (v/v) formaldehyde) and dehydrated through a graded ethanol series. The end of fibers closest to ovules were embedded in paraffin with ceresin and sliced into 10-μm thick cross-sections with a rotary microtome (Reichert-Histo stat, Germany) as published (Avci et al., 2013). Cell walls were separately stained by 0.01% (w/v) calcofluor white and 0.1% (w/v) direct red 23 dyes as described previously (Brill et al., 2011; Huang et al., 2021). The stained sections were observed under a confocal laser scanning microscope (LSM710, Zeiss, Oberkochen, Germany).

VIGS experiment

For VIGS, a previously published method was followed (Gu et al., 2014). The cDNA sequences for each TF gene were amplified by PCR and ligated into pCLCrV-A digested with SpeI. The *Magnesium chelatase subunit I* (*CHLI*) gene was used as a positive control. The plasmids pCLCrV-A, pCLCrV-B, and pCLCrV-CHLI500 were individually transformed into Agrobacterium strain GV3101. The Agrobacterium cell was suspended to an OD_{600} (optical density at 600 nm) of 1 and then was injected into cotton cotyledons. A total of 20 cotton bolls from WT and VIGS plants were investigated.

Accession numbers

The RNA-seq data related to this research were deposited at NCBI SRA, which can be found under following accession numbers: PRJNA870699 and PRJNA871199. The gene sequence data from this article can be found in the Cotton Functional Genomics Database (https://cottonfgd.net/) under the following accession numbers: *GhCesA8*, Ghir_D10G004060; *GhCesA4*, Ghir_A08G005110; *GhCesA7-1*, Ghir_D07G004340; *GhCesA7-2*, Ghir_A05G000980; *GhKCS57*, Gh_A01G0006; *GhKCS5*, Ghir_D02G017570.1; *GhKCS13*, Ghir_D01G019360.1; *GhKCS23*, Ghir_D10G015750.1; *GhGA20OX1*, Ghir_A10G012140; *GhGA3OX1*, Ghir_A10G007560.1; *GhD27*, Gh_D07G2115; *GhMAX3*, Ghir_D12G010530; *GhMAX4*, Ghir_D07G002670; *GhMAX1*, Ghir_D05G004440; *GhB9SHZ1*, Gh_A05G0747; *GhNAC100-2*, Gh_D11G2467; *GhGT2*, Gh_A05G2067; *GhBLH51*, Gh_D10G2406; *GhGRF4*, CotAD_02895.

Supplemental data

The following materials are available in the online version of this article.

Supplemental Figure S1. Relative expression levels of SL biosynthesis genes in fiber cells at different developmental stages.

Supplemental Figure S2 Genome-wide analysis of the *GhD27* gene family and their expression profiling in fiber cell and other various tissues.

Supplemental Figure S3. Genotyping of transgenic cotton lines overexpressing *GhD27* (*GhD27*-OE lines).

Supplemental Figure S4. Relative expression levels of *GhD27* genes in fibers from the D-subgenome (A) and A-subgenome (B) of WT and *Ghd27-ko* transgenic cotton.

Supplemental Figure S5. *epi*-5DS contents in 25-DPA cotton fibers collected from WT, *GhD27*-OE (A), and *Ghd27-ko* (B) lines.

Supplemental Figure S6. Phenotypic analysis of the whole plants of WT and *Ghd27-ko* transgenic cottons.

Supplemental Figure S7. Phenotypic analysis (A) and length measurement (B) of WT fibers and *Ghd27-ko* fibers cultured *in vitro* with or without GR24.

Supplemental Figure S8. Analysis of DEGs in fiber cells after GR24 or Tis108 treatment.

Supplemental Figure S9. Cell wall thickness of cells untreated (Con) fiber and fiber cells treated with either GR24 or Tis108.

Supplemental Figure S10. Comparison analysis of fiber cell wall thickness from WT, *GhD27*-OE, and *Ghd27-ko* transgenic cottons.

Supplemental Figure S11. Comparison analysis of fiber cell wall thickness from WT, *GhD27*-OE, and *Ghd27-ko* transgenic plants.

Supplemental Figure S12. Transcriptome data showing the relative expression levels of *GhCesA4*, *GhCesA8*, *GhCesA7-1*, and *GhCesA7-2* in fibers from *GhD27*-OE and *Ghd27-ko* lines.

Supplemental Figure S13. Cellulose content and expression level of SLs biosynthetic genes in fibers untreated and treated with cellulose biosynthesis inhibitor DCB and coumarin.

Supplemental Figure S14. Systematic Y1H assay to identify the SL-inducible TFs capable of binding to the promoters of *CesA* genes responsible for cellulose biosynthesis.

Supplemental Figure S15. Relative expression levels of *GhB9SHZ1* and *GhGT2* upon treatment of GR24 or Tis108 for 5, 10, 15, or 20 days.

Supplemental Figure S16. Quantification of LUC activity from the dual-LUC assays in Figure 5B.

Supplemental Figure S17. Systematic Y1H assays to identify the binding sites of *GhCesA8* and *GhCesA7-2* promoters by the TFs GhB9SHZ1.

Supplemental Figure S18. Systematic Y1H assays to identify the binding sites of *GhCesA7-1* promoter by the TFs GhGT2.

Supplemental Figure S19. Systematic Y1H assay to identify the SL-inducible TFs capable of binding to the promoters of *KCS* genes essential for VLCFA biosynthesis.

Supplemental Figure S20. Relative expression levels of *GhBLH51* and *GhNAC100-2* in fiber cells upon the treatment of GR24 or Tis108 for 5, 10, 15, or 20 days.

Supplemental Figure S21. Quantification of LUC activity for the dual-LUC assays in Figure 5H.

Supplemental Figure S22. Systematic Y1H assays to identify the binding sites in the *GhKCS5* promoter by the TFs GhBLH51 or GhNAC100-2.

Supplemental Figure S23. Systematic Y1H assays to identify the binding sites in the *GhKCS23* promoter by the TFs GhGT2 and GhNAC100-2.

Supplemental Figure S24. Relative expression levels of *GhB9SHZ1*, *GhBLH51*, *GhNAC100-2*, and *GhGT2* in fibers of WT, *GhD27*-OE, and *Ghd27-ko* transgenic cotton plants.

Supplemental Figure S25. Comparison of fiber cell wall thickness of WT, nonsilenced, *GhB9SHZ1*-silenced and *GhGT2*-silenced cotton plants.

Supplemental Figure S26. Statistical analysis of fiber lengths of WT, vector control plants and *GhBLH51*-, *GhNAC100-2*-, *GhGT2*-silenced plants.

Supplemental Figure S27. Fiber length in Figure 9A.

Supplemental Figure S28. The effect of GA_3 or PAC on the development of fibers from WT, *GhD27*-OE and *Ghd27-ko* transgenic cotton plants.

Supplemental Figure S29. Relative expression levels of SL biosynthesis genes (*GhMAX1*, *GhMAX3*, and *GhMAX4*) upon the treatment of 1 μM GA_3 or 5 μM PAC for 10, 15, or 20 days.

Supplemental Figure S30. Systematic Y1H assay to identify the GA-inducible TFs capable of binding to the promoters of the key SL biosynthesis gene *GhD27*.

Supplemental Figure S31. Global analysis of the *GhGRF* gene family and their expression profiling in fibers and other various tissues.

Supplemental Figure S32. Relative expression levels of *GhGRF4* upon treatment with 1 μM GA_3 or 5 μM PAC for 5, 10, 15, or 20 days.

Supplemental Figure S33. Nucleotide sequence of the intact *GhD27* promoter fragment and mutated *GhD27* promoter fragments carrying mutation at GRF-binding sites shown in Figure 9L, used for the Y1H assay in Figure 9M.

Supplemental Figure S34. Sanger sequencing-based genotyping of *GhGRF4*-knockout lines obtained by CRISPR/Cas9 gene editing.

Supplemental Figure S35. Relative expression levels of *GhGRF4* genes from the D-subgenome (A) and A-subgenome (B) in fibers of WT and *Ghgrf4-ko* transgenic plants.

Supplemental Figure S36. Comparison of cell wall thickness of fibers from WT, nonsilenced and *Ghgrf4-ko* cotton plants.

Supplemental Table S1. Detailed information of genes enriched in cell wall term.

Supplemental Table S2. TF genes upregulated upon GR24 treatment and downregulated upon Tis108 treatment.

Supplemental Table S3. Analysis of 15 upregulated TF genes in GA acid treated ovules

Supplemental Data Set 1. Detailed list of genes that upregulated after rac-GR24 treatment compared to Tis108 treatment.

Supplemental Data Set 2. Detailed list of genes enriched in fatty acid term.

Supplemental Data Set 3. Primers used in this study.

Supplemental Data Set 4. Summary of statistical analyses.

Supplemental File S1. Multiple protein sequence alignment used to generate the phylogenetic tree shown in Supplemental Figure S2.

Supplemental File S2. Newick file format of the phylogenetic tree shown in Supplemental Figure S2.

Supplemental File S3. Multiple protein sequence alignment used to generate the phylogenetic tree shown in Supplemental Figure S31.

Supplemental File S4. Newick file format of the phylogenetic tree shown in Supplemental Figure S31.

Acknowledgments

We thank Prof. Jianing Yu for constructive comments.

Funding

This work was supported by the National Natural Science Foundation of China (32070549), Shaanxi Youth Entrusted Talent Program (20190205), Fundamental Research Funds for the Central Universities (GK202002005 and GK202201017), Young Elite Scientists Sponsorship Program by China Association for Science and Technology (CAST) (2019-2021QNRC001), State Key Laboratory of Cotton Biology Open Fund (CB2020A12 and CB2021A21) and FWF Stand-alone Project (P29988).

Conflict of interest statement. The authors declare no competing interests.

References

Agusti J, Herold S, Schwarz M, Sanchez P, Ljung K, Dun EA, Brewer PB, Beveridge CA, Sieberer T, Sehr EM, et al. (2011) Strigolactone signaling is required for auxin-dependent stimulation of secondary growth in plants. Proc Natl Acad Sci USA **108**: 20242–20247

Anderson CT, Kieber JJ (2020) Dynamic construction, perception, and remodeling of plant cell walls. Ann Rev Plant Biol **71**: 39–69

Avci U, Pattathil S, Singh B, Brown V, Hahn M, Haigler C (2013) Cotton fiber cell walls of *Gossypium hirsutum* and *Gossypium barbadense* have differences related to loosely-bound xyloglucan. PLoS One **8**: e56315

Bai WQ, Xiao YH, Zhao J, Song SQ, Hu L, Zeng JY, Li XB, Hou L, Luo M, Li DM, et al. (2014) Gibberellin overproduction promotes sucrose synthase expression and secondary cell wall eeposition in cotton fibers. PLoS One **9**: e96537

Besserer A, Bécard G, Jauneau A, Roux C, Séjalon-Delmas N (2008) GR24, a synthetic analog of strigolactones, stimulates the mitosis and growth of the arbuscular mycorrhizal fungus Gigaspora rosea by boosting its energy metabolism. Plant Physiol **148**: 402–413

Bindea G, Mlecnik B, Hackl H, Charoentong P, Tosolini M, Kirilovsky A, Fridman WH, Pagès F, Trajanoski Z, Galon J (2009) ClueGO: a cytoscape plug-in to decipher functionally grouped gene ontology and pathway annotation networks. Bioinformatics **25**: 1091–1093

Brewer P, Koltai H, Beveridge CA (2013) Diverse roles of strigolactones in plant development. Mol Plant **6**: 18–28

Brill E, van Thournout M, White R, Llewellyn D, Campbell P, Engelen S, Ruan Y, Arioli T, Furbank R (2011) A novel isoform of sucrose synthase is targeted to the cell wall during secondary cell wall synthesis in cotton fiber. Plant Physiol **157**: 40–54

Cao JF, Zhao B, Huang CC, Chen ZW, Zhao T, Liu HR, Hu GJ, Shangguan XX, Shan CM, Wang LJ, et al. (2020) The miR319-targeted GhTCP4 promotes the transition from cell elongation to wall thickening in cotton fiber. Mol Plant **13**: 1063–1077

Chen S, Zhou Y, Chen Y, Gu J (2018) fastp: an ultra-fast all-in-one FASTQ preprocessor. Bioinformatics **34**: 884–890

Cook CE, Whichard LP, Turner B, Wall ME, Egley GH (1966) Germination of witchweed (*striga lutea* lour.): isolation and properties of a potent stimulant. Science **154**: 1189–1190

Cosgrove DJ, Jarvis MC (2012) Comparative structure and biomechanics of plant primary and secondary cell walls. Front Plant Sci **3**: 204

Duan J, Yu H, Yuan K, Liao Z, Meng X, Jing Y, Liu G, Chu J, Li J (2019) Strigolactone promotes cytokinin degradation through transcriptional activation of CYTOKININ OXIDASE/DEHYDROGENASE 9 in rice. Proc Natl Acad Sci USA **116**: 14319–14324

Gigli-Bisceglia N, Engelsdorf T, Hamann T (2020) Plant cell wall integrity maintenance in model plants and crop species-relevant cell wall components and underlying guiding principles. Cell Mol Life Sci **77**: 2049–2077

Gomez-Roldan V, Fermas S, Brewer PB, Puech-Pagès V, Dun EA, Pillot JP, Letisse F, Matusova R, Danoun S, Portais JC, et al. (2008) Strigolactone inhibition of shoot branching. Nature **455**: 189–194

Gou JY, Wang LJ, Chen SP, Hu WL, Chen XY (2007) Gene expression and metabolite profiles of cotton fiber during cell elongation and secondary cell wall synthesis. Cell Res **17**: 422–434

Gu Z, Huang C, Li F, Zhou X (2014) A versatile system for functional analysis of genes and microRNAs in cotton. Plant Biotechnol J **12**: 638–649

Haigler C, Betancur L, Stiff M, Tuttle J (2012) Cotton fiber: a powerful single-cell model for cell wall and cellulose research. Front Plant Sci **3**: 104

Hamant O, Traas J (2010) The mechanics behind plant development. New Phytologist **185**: 369–385

Hossain MS, Joshi T, Stacey G (2015) System approaches to study root hairs as a single cell plant model: current status and future perspectives. Front Plant Sci **6**: 1–7

Houston K, Tucker MR, Chowdhury J, Shirley N, Little A (2016) The plant cell wall: a complex and dynamic structure as revealed by the responses of genes under stress conditions. Front Plant Sci **7**: 984

Hu Y, Chen J, Fang L, Zhang Z, Ma W, Niu Y, Ju L, Deng J, Zhao T, Lian J, et al. (2019) *Gossypium barbadense* and *Gossypium hirsutum* genomes provide insights into the origin and evolution of allotetraploid cotton. Nat Genetics **51**: 739–748

Huang G, Huang JQ, Chen XY, Zhu YX (2021) Recent advances and future perspectives in cotton research. Ann Rev Plant Biol **72**: 437–462

Huang JF, Chen F, Guo YJ, Gan XL, Yang MM, Zeng W, Persson S, Xu WL (2021) GhMYB7 promotes secondary wall cellulose deposition in cotton fibers by regulating *GhCesA* gene expression through three distinct cis-elements. New Phytologist **232**: 1718–1737

Huang JF, Chen F, Wu SY, Li J, Xu WL (2016) Cotton GhMYB7 is predominantly expressed in developing fibers and regulates secondary cell wall biosynthesis in transgenic Arabidopsis. Sci China Life Sci **59**: 194–205

Hülskamp M (2004) Plant trichomes: a model for cell differentiation. Nat Rev Mol Cell Biol **5**: 471–480

Ito S, Umehara S, Hanada A, Yamaguchi S, Asami T (2013) Effects of strigolactone-biosynthesis inhibitor TIS108 on Arabidopsis. Plant Signal Behav **8**: e24193

Ito S, Yamagami D, Umehara M, Hanada A, Yoshida S, Sasaki Y, Yajima S, Kyozuka J, Ueguchi-Tanaka M, Matsuoka M, et al. (2017) Regulation of strigolactone biosynthesis by gibberellin signaling. Plant Physiol **174**: 1250–1259

Jiang L, Liu X, Xiong G, Liu H, Chen F, Wang L, Meng X, Liu G, Yu H, Yuan Y, et al. (2013) DWARF 53 acts as a repressor of strigolactone signalling in rice. Nature **504**: 401–405

Kanno Y, Oikawa T, Chiba Y, Ishimaru Y, Shimizu T, Sano N, Koshiba T, Kamiya Y, Ueda M, Seo M (2016) AtSWEET13 and AtSWEET14 regulate gibberellin-mediated physiological processes. Nat Commun **7**: 13245

Kapulnik Y, Delaux PM, Resnick N, Mayzlish-Gati E, Wininger S, Bhattacharya C, Séjalon-Delmas N, Combier JP, Bécard G, Belausov E, et al. (2011) Strigolactones affect lateral root formation and root-hair elongation in Arabidopsis. Planta **233**: 209–216

Khosla A, Nelson DC (2016) Strigolactones, super hormones in the fight against Striga. Curr Opin Plant Biol **33**: 57–63

Kim D, Langmead B, Salzberg SL (2015) HISAT: a fast spliced aligner with low memory requirements. Nat Methods **12**: 357–360

Kim HJ, Triplett BA (2001) Cotton fiber growth in planta and in vitro. Models for plant cell elongation and cell wall biogenesis. Plant Physiol **127**: 1361–1366

Koltai H, Dor E, Hershenhorn J, Joel DM, Weininger S, Lekalla S, Shealtiel H, Bhattacharya C, Eliahu E, Resnick N, et al. (2010) Strigolactones' effect on root growth and root-hair elongation may be mediated by auxin-efflux carriers. J Plant Growth Regul **29**: 129–136

Langmead B, Salzberg SL (2012) Fast gapped-read alignment with Bowtie 2. Nat Methods **9**: 357–359

Lantzouni O, Alkofer A, Falter-Braun P, Schwechheimer C (2020) GROWTH-REGULATING FACTORS interact with DELLAs and regulate growth in cold stress. Plant Cell **32**: 1018–1034

Li F, Fan G, Lu C, Xiao G, Zou C, Kohel RJ, Ma Z, Shang H, Ma X, Wu J, et al. (2015) Genome sequence of cultivated Upland cotton (*Gossypium hirsutum* TM-1) provides insights into genome evolution. Nat Biotechnol **33**: 524–530

Li FF, Wu SJ, Chen TZ, Zhang J, Wang HH, Guo WZ, Zhang TZ (2009) Agrobacterium-mediated co-transformation of multiple genes in upland cotton. Plant Cell Tissue Organ Culture **97**: 225–235

Liu GJ, Xiao GH, Liu NJ, Liu D, Chen PS, Qin YM, Zhu YX (2015) Targeted lipidomics studies reveal that linolenic acid promotes cotton fiber elongation by activating phosphatidylinositol and phosphatidylinositol monophosphate biosynthesis. Mol Plant **8**: 911–921

Livak KJ, Schmittgen TD (2001) Analysis of relative gene expression data usingreal-time quantitative PCR and the 2 $-\Delta\Delta$CT method. Methods **25**: 402–408

Love MI, Huber W, Anders S (2014) Moderated estimation of fold change and dispersion for RNA-seq data with DESeq2. Genome Biol **15**: 550

Martínez-Rubio R, Acebes JL, Encina A, Kärkönen A (2018) Class III peroxidases in cellulose deficient cultured maize cells during cell wall remodeling. Physiol Plant **164**: 45–55

Mashiguchi K, Seto Y, Yamaguchi S (2021) Strigolactone biosynthesis, transport and perception. Plant J **105**: 335–350

Nakamura H, Xue YL, Miyakawa T, Hou F, Qin HM, Fukui K, Shi X, Ito E, Ito S, Park SH, et al. (2013) Molecular mechanism of strigolactone perception by DWARF14.Nat Commun **4**: 3613

Niu Q, Tan K, Zang Z, Xiao Z, Chen K, Hu M, Luo M (2019) Modification of phytosterol composition influences cotton fiber cell elongation and secondary cell wall deposition. BMC Plant Biol **19**: 208

Oh CS, Toke DA, Mandala S, Martin CE (1997) *ELO2* and *ELO3*, homologues of the *Saccharomyces cerevisiae ELO1* gene, function in fatty acid elongation and are required for sphingolipid formation. J Biol Chem **272**: 17376–17384

Pang CY, Wang H, Pang Y, Xu C, Jiao Y, Qin YM, Western TL, Yu SX, Zhu YX (2010) Comparative proteomics indicates that biosynthesis of pectic precursors is important for cotton fiber and Arabidopsis root hair elongation. Mol Cell Proteom **9**: 2019–2033

Pertea M, Pertea GM, Antonescu CM, Chang TC, Mendell JT, Salzberg SL (2015) StringTie enables improved reconstruction of a transcriptome from RNA-seq reads. Nat Biotechnol **33**: 290–295

Polko JK, Kieber JJ (2019) The regulation of cellulose biosynthesis in plants. Plant Cell **31**: 282–296

Purushotham P, Ho R, Zimmer J (2020) Architecture of a catalytically active homotrimeric plant cellulose synthase complex. Science **369**: 1089–1094

Qin YM, Hu CY, Pang Y, Kastaniotis AJ, Hiltunen JK, Zhu YX (2007) Saturated very-long-chain fatty acids promote cotton fiber and Arabidopsis cell elongation by activating ethylene biosynthesis. Plant Cell **19**: 3692–3704

Rasmussen A, Mason MG, de Cuyper C, Brewer PB, Herold S, Agusti J, Geelen D, Greb T, Goormachtig S, Beeckman T, et al. (2012) Strigolactones suppress adventitious rooting in arabidopsis and pea. Plant Physiol **158**: 1976–1987

Sampedro J, Cosgrove DJ (2005) The expansin superfamily. Genome Biol **6**: 242

Seto Y, Sado A, Asami K, Hanada A, Umehara M, Akiyama K, Yamaguchi S (2014) Carlactone is an endogenous biosynthetic precursor for strigolactones. Proc Natl Acad Sci USA **111**: 1640–1645

Shan CM, Shangguan XX, Zhao B, Zhang XF, Chao LM, Yang CQ, Wang LJ, Zhu HY, Zeng Y Da, Guo WZ, et al. (2014) Control of cotton fibre elongation by a homeodomain transcription factor GhHOX3. Nat Commun **5**: 5519

Shi YH, Zhu SW, Mao XZ, Feng JX, Qin YM, Zhang L, Cheng J, Wei LP, Wang ZY, Zhu YX (2006) Transcriptome profiling, molecular biological., and physiological studies reveal a major role for ethylene in cotton fiber cell elongation. Plant Cell **18**: 651–664

Sun Y, Veerabomma S, Abdel-Mageed HA, Fokar M, Asami T, Yoshida S, Allen RD (2005) Brassinosteroid regulates fiber development on cultured cotton ovules. Plant Cell Physiol **46**: 1384–1391

Tausif M, Jabbar A, Naeem MS, Basit A, Ahmad F, Cassidy T (2018) Cotton in the new millennium: advances, economics, perceptions and problems. Textile Prog **50**: 1–66

Toke DA, Martin CE (1996) Isolation and characterization of a gene affecting fatty acid elongation in Saccharomyces cerevisiae. J Biol Chem **271**: 18413–18422

Umehara M, Hanada A, Yoshida S, Akiyama K, Arite T, Takeda-Kamiya N, Magome H, Kamiya Y, Shirasu K, Yoneyama K, et al. (2008) Inhibition of shoot branching by new terpenoid plant hormones. Nature **455**: 195–200

Vanstraelen M, Benková E (2012) Hormonal interactions in the regulation of plant development. Ann Rev Cell Dev Biol **28**: 463–487

Wang X, Guan Y, Zhang D, Dong X, Tian L, Qing Q (2017) A β-Ketoacyl-CoA synthase is involved in rice leaf cuticular wax synthesis and requires a CER2-LIKE protein as a cofactor. Plant Physiol **173**: 944–955

Xiao G, Zhao P, Zhang Y (2019) A pivotal role of hormones in regulating cotton fiber development. Front Plant Sci **10**: 87

Xiao GH, Wang K, Huang G, Zhu YX (2016) Genome-scale analysis of the cotton *KCS* gene family revealed a binary mode of action for gibberellin A regulated fiber growth. J Integr Plant Biol **58**: 577–589

Xiao YH, Li DM, Yin MH, Li XB, Zhang M, Wang YJ, Dong J, Zhao J, Luo M, Luo XY, et al. (2010) Gibberellin 20-oxidase promotes initiation and elongation of cotton fibers by regulating gibberellin synthesis. J Plant Physiol **167**: 829–837

Yang C, Ye Z (2013) Trichomes as models for studying plant cell differentiation. Cell Mol Life Sci **70**: 1937–1948

Yang Z, Zhang C, Yang X, Liu K, Wu Z, Zhang X, Zheng W, Xun Q, Liu C, Lu L, et al. (2014) PAG1, a cotton brassinosteroid catabolism gene, modulates fiber elongation. New Phytologist **203**: 437–448

Zeng J, Zhang M, Hou L, Bai W, Yan X, Hou N, Wang H, Huang J, Zhao J, Pei Y (2019) Cytokinin inhibits cotton fiber initiation by disrupting PIN3a-mediated asymmetric accumulation of auxin in the ovule epidermis. J Exp Bot **70**: 3139–3151

Zhang J, Mazur E, Balla J, Gallei M, Kalousek P, Medved'ová Z, Li Y, Wang Y, Prát T, Vasileva M, et al. (2020) Strigolactones inhibit auxin feedback on PIN-dependent auxin transport canalization. Nat Commun **11**: 3508

Zhong R, Cui D, Ye ZH (2019) Secondary cell wall biosynthesis. New Phytologist **221**: 1703–1723